The Effect of the El Nino Southern Oscillation on U.S. Corn Production and Downside Risk

Jesse B. Tack [*†]
PO Box 5187
Mississippi State, MS 39762
Phone: (662) 325-7999
Fax: (662) 325-8777
E-Mail: tack@agecon.msstate.edu

David Ubilava [‡]
PO Box 5187
Mississippi State, MS 39762
Phone: (662) 325-2676
Fax: (662) 325-8777
E-Mail: ubilava@agecon.msstate.edu

Selected Paper prepared for presentation at the Southern Agricultural Economics Association Annual Meeting, Birmingham, AL, February 4–7, 2012

[*]Corresponding Author.
[†]Assistant Professor. Department of Agricultural Economics, Mississippi State University.
[‡]Post-Doctoral Research Associate. Department of Agricultural Economics, Mississippi State University.

The Effect of the El Nino Southern Oscillation on U.S. Corn Production and Downside Risk

Abstract

El Niño Southern Oscillation (ENSO) teleconnections imply anomalous weather conditions around the globe, causing yield shortages, price changes, and even civil unrests. Extreme ENSO events may cause catastrophic damages to crop yields, thus amplifying downside risk for producers. This study presents a framework for quantifying the effects of climate on crop yield distributions. An empirical application provides estimates of the effect that ENSO events have on the means of U.S. county-level corn yield distributions, as well as the probabilities of catastrophic crop loss. Our findings demonstrate that ENSO events strongly influence these probabilities systematically over large production regions, which has important implications for research and policy analysis in the production, risk management, climate change, and civil unrest literatures.

Keywords: Climate, El Niño Southern Oscillation, Maximum Entropy, Risk Management, Yield Distribution

1 Introduction

El Niño Southern Oscillation (ENSO) is a climatic phenomenon that takes place in the tropical Pacific and has global weather implications (Ropelewski and Halpert, 1987; Kiladis and Diaz, 1989; Rasmusson, 1991; Adams et al., 1999). ENSO has the potential to affect world economies, amplify social instabilities and may even provoke civil wars in different parts of the world (Handler, 1990; Solow et al., 1998; Brunner, 2002; Hsiang et al., 2011). In fact, researchers have speculated that ENSO is responsible for such historically documented events as the biblical droughts in Egypt (Eltahir, 1996), and the demise of ancient civilizations (Haug et al., 2003; Tsonis et al., 2010). Linking climatic events to the world socio–political environment is not as paradoxical as it may first sound, a reasonable causal mechanism being weather's effect on agricultural production and thus food prices (Bellemare, 2011), which is, in turn, causally linked to social unrest.

While weather's connection to civil war and the demise of civilizations has not been widely established, there exists clear-cut justifications for linking large-scale medium-frequency weather events with economic variables. This has generated much interest in studying the role of ENSO on various measures of economic performance (Brunner, 2002; Kim and McCarl, 2005). Particular attention has been paid to the causal relationship between ENSO and agricultural and fish production and management (e.g. Handler, 1990; Carlson et al., 1996; Hansen et al., 1998; Adams et al., 1999; Legler et al., 1999; Dalton, 2001).

El Niño is one of two extreme ENSO events, during which trade winds across the tropical Pacific weaken, resulting in unusually warm sea surface temperatures in the region. The counterpart of El Niño is La Niña, which is associated with very intense trade winds and colder-than-normal sea surface temperatures. These extreme events have the potential to impact agriculture through multiple vectors. First, ENSO linkages with precipitation and temperature provide a straightforward causal connection with crop production. Second, extreme ENSO events are likely to amplify hazardous weather conditions, resulting in damaging storms, drought, and flooding. Lastly, climate conditions during ENSO events are correlated with pest damage as extreme conditions can generate large changes in development rates for insects and germination rates for bacteria, fungi, and nematodes (Rosenzweig et al., 2000; Iglesias and Rosenzweig, 2007).

Among other regions, the U.S. is greatly affected by ENSO events. Previous research has linked ENSO with precipitation and temperature patterns in different regions (Ropelewski and Halpert, 1986; Stone et al., 1996; Montroy, 1997; Barlow et al., 2001). Thus far, studies have found meaningful connections between La Niña and droughts in the Western Corn Belt (Handler and Handler, 1983; Handler, 1984, 1990), and increased probabilities of damaging storms and hurricanes in the Southeast (Bove et al., 1998; Saunders et al., 2000). On the other hand, El Niño events have been linked to hotter and drier climate, with increased probabilities of wildfires in the Southeastern U.S. (Swetnam and Betancourt, 1990; Brenner, 1991; Legler et al., 1999).

El Niño and La Niña can impact U.S. agriculture through multiple vectors. First, ENSO linkages with precipitation and temperature provide a straightforward causal connection with crop production. Second, extreme ENSO events are likely to amplify hazardous weather conditions,

resulting in damaging storms, drought, and flooding. Lastly, climate conditions during ENSO events are correlated with pest damage as extreme conditions can generate large changes in development rates for insects and germination rates for bacteria, fungi, and nematodes (Rosenzweig et al., 2000; Iglesias and Rosenzweig, 2007).

Understanding the effects of ENSO is becoming increasingly important as the frequency and intensity of events will likely increase parallel to climate change (Timmermann et al., 1999; Chen et al., 2008). In the short run, effects of ENSO events can be measured as their immediate impact on crop yields. Several papers have analyzed the economic impact of extreme ENSO events, and found that both El Niño and La Niña have potentially damaging implications for U.S. agriculture (Solow et al., 1998; Adams et al., 1999; Chen et al., 2002). In the intermediate run, amplified ENSO conditions associated with climate change may call for adaptive actions by crop producers, in order to avoid falling into the trap of a "dumb farmer" and not updating production techniques (Kelly et al., 2005). A better understanding of ENSO events and their effects on crop production could potentially help mitigate losses associated with climate change, and could result in annual welfare gains of several hundred million U.S. dollars (Chen et al., 2001).

Previous research linking ENSO events to crop production has focused on implications for the mean of the crop yield distribution. This approach is potentially limiting in that it does not take into account ENSO's effect on the overall shape of the distribution (Chen et al., 2004). The importance of the distribution's shape for agricultural production and downside risk management is well established (Chavas and Holt, 1996; Moschini and Hennessy, 2001; Antle, 2010). In addition, mitigation of downside risk is the dominant driver of nearly all agricultural policy instruments, whose efficiencies rely on accurate knowledge of the lower tail of the yield distribution. Lastly, recent research suggests that food price increases (rather than food price volatility) leads to increased social unrest (Barrett and Bellemare, 2011; Bellemare, 2011). To the extent that crops are storable, price spikes are likely to be triggered by widespread crop losses, which suggests that the lower tail of the yield distribution could be part of the causal chain linking ENSO events to social unrest.

The objective of this research is to analyze the effects of extreme ENSO occurrences on corn yield distributions. We focus on the U.S. as it is the global leader in corn production, and recent

interest in corn-based ethanol has further amplified the importance of this crop. As the U.S. is also the world's largest corn exporter, ENSO's effect on U.S. production has global implications. We hypothesize that yield distributions under alternative ENSO regimes are different in two important ways: (i) the mean of the distribution and (ii) the downside risk captured by the density in the lower tail of the distribution. We allow for these distributions to be nonlinear functions of ENSO events and allow for asymmetries across El Niño and La Niña events. This flexibility is consistent with recent findings in the climate literature suggesting nonlinearities in both ENSO dynamics and its linkages with weather events (Noel and Changnon, 1998; Hall et al., 2001). Finally, based on the findings of Chen, McCarl, and Schimmelpfennig (Chen et al., 2004), we allow for spatial heterogeneity of ENSO effects on crop production across a large panel of U.S. counties. This represents a considerable downsizing in observational units relative to more common state- and country-level approaches, and provides a fuller representation of spatial effects.

Our findings reveal important relationships between ENSO events and corn yields, have important implications for researchers and policy makers in a broad range of disciplines including crop production, risk management, climate change, and civil unrest. Consistent with the expectations this relationship extends to the higher order moments of corn yield distribution, suggesting that ENSO does impact the downside risk. Moreover, we observe both asymmetries and spatial heterogeneity of ENSO effect on yield distribution, once again emphasizing the intricate nature of the ENSO phenomenon. In what follows, we will first present the empirical framework for this research. Next, we describe the data and then discuss the empirical results and implications. Finally, we summarize our main findings and discuss the big picture contributions of this research.

2 Empirical Framework

We utilize a similar empirical framework for linking climate variables to agricultural production as Tack, Harri, and Coble (Tack et al., 2011), which extended the modeling approach of Schlenker and Roberts (Schlenker and Roberts, 2006, 2009) by considering higher order moments of the yield distribution. We further extend the Tack, Harri, and Coble model by directly controlling for El Niño and La Niña events within the regression framework, which provides additional vectors beyond

temperature and precipitation for ENSO events to affect yield outcomes. This is an important adaptation relative to previous models linking ENSO to crop yields as it controls for the effect of complicated interactions among hazardous weather conditions and environmental pests.

Our approach has two components, and each is described in the following two subsections. The first component utilizes a data-based regression framework to predict raw moments of the yield distribution under three ENSO regimes: El Niño, La Niña, and Neutral (we discuss how we distinguish between these three regimes in the Data section below). The second component utilizes these predicted moments within a maximum entropy framework to identify how the El Niño and La Niña regimes perturb the distribution of yields relative to the Neutral regime. This allows us to quantify the magnitude of the El Niño and La Niña effects on the mean of the yield distribution, as well as producers' exposure to downside risk.

Another point of departure between our method is that we utilize centered moments in the maximum entropy framework, whereas the Tack, Harri, and Coble approach utilized raw moments. The reason for this departure is twofold. First, the mean, variance, and skewness of crop yields have been the focus of much of the distribution modeling literature (Day, 1965; Gallagher, 1987; Nelson and Preckel, 1989; Moss and Shonkwiler, 1993; Goodwin and Ker, 1998; Ker and Coble, 2003; Ramirez et al., 2003; Sherrick et al., 2004; Hennessy, 2009a,b). Second, it is likely that centered moments create more stable constraints within the maximum entropy framework relative to raw moments, whose values get (necessarily) exponentially larger for higher order moments. Centered moments also have this feature, but the growth is much slower given that they are constructed using deviations rather than levels.

2.1 Modeling Higher Order Moments

The empirical model for the $j = 1, ..., J$ raw moments of the corn yield distribution is

$$\begin{aligned} y_{ist}^{j} &= \alpha_{ij} + \beta_{js1} low_{it} + \beta_{js2} med_{it} + \beta_{js3} high_{it} + \beta_{js4} prec_{it} + \beta_{js5} prec_{it}^{2} \\ &\quad + \beta_{js6} nino_{t} + \beta_{js7} nina_{t} + \beta_{js8} trend_{it} + \varepsilon_{ijt} \end{aligned} \tag{1}$$

where the dependent variable y_{ist}^{j} is the j^{th} power of the yield variable for county i in state s in period t, α_{ij} is a county-by-equation fixed effect, low_{it} captures the intensity of low temperatures experienced during the growing season, med_{it} captures the intensity of medium temperatures, and $high_{it}$ captures the intensity of high temperatures. We include a quadratic effect for precipitation, and two dummy variables $nino_{it}$ and $nina_{it}$ that are equal to one if an El Niño or La Niña event was experienced during the growing season. We also include an equation specific linear trend to control for technological change over time. Note that we have allowed the parameters to vary by state, as we will estimate this model for each state in our data.

Under the assumption $E\left(\varepsilon_{ijt}\right) = 0$ the equations in (1) can be thought of as directly formulating how climate and technological change affect moments of the crop yield distribution. The authors point out that one can consistently estimate these moments using ordinary least squares techniques (Tack et al., 2011).

2.2 Regime Specific Distributions

While the parameters in equation (1) capture the causal relationship of climate and technological change with the higher order moments of the yield distribution, it is not immediately clear how these variables affect the overall shape of the distribution. The ability to predict the moments under different regimes does not in and of itself allow us to measure the effect of these regimes on the entire distribution of yield outcomes (Tack et al., 2011). The inability of a finite set of moments to determine the entire density is often referred to as the moments problem (Shohat and Tamarkin, 1943), and previous work in the yield modeling literature has demonstrated how this problem can be ameliorated using the concept of maximum entropy (Stohs, 2003; Tack et al., 2011).

Define by $\mu_{ij} \equiv E\left(Y_i^j\right)$ the j^{th} raw moment of the random variable Y_i, the yield for county i. Also define by $\mathbf{X}_i$ a county specific random vector for the right-hand side variables of equation (1) and define the outcomes $\mathbf{x}_i^{nino}$, $\mathbf{x}_i^{nina}$, and $\mathbf{x}_i^{neutral}$ as values for the right-hand side variables that represent the El Niño, La Niña, and Neutral regimes. We define the raw moments conditional on these outcomes as $\mu_{ij}^{nino} \equiv \left(Y_i^j \mid \mathbf{X}_i = \mathbf{x}_i^{nino}\right)$, $\mu_{ij}^{nina} \equiv E\left(Y_i^j \mid \mathbf{X}_i = \mathbf{x}_i^{nina}\right)$, and $\mu_{ij}^{neutral} \equiv E\left(Y_i^j \mid \mathbf{X}_i = \mathbf{x}_i^{neutral}\right)$.

For an arbitrary county i and regime $r \in \{nino, nina, neutral\}$, the maximum entropy distribution is defined by

$$f_{ir}^{*} = \arg\max_{f} - \int f(y) \ln f(y) \, dy \tag{2}$$

subject to the moment constraints

$$\int f(y) \, dy = 1 \text{ and } \int y^{j} f(y) \, dy = \mu_{ij}^{r}, j = 1, \ldots, J. \tag{3}$$

The associated Lagrangian for this maximization problem is

$$\mathcal{L} = - \int f(y) \ln f(y) \, dy - \gamma_0 \left[\int f(y) \, dy - 1 \right] - \sum_{j=1}^{J} \gamma_j \left[\int y^{j} f(y) \, dy - \mu_{ij}^{r} \right] \tag{4}$$

and the implied solution is the maximum entropy density

$$\begin{aligned} f_{ir}^{*}(y) &= \frac{1}{\psi(\gamma_{ir}^{*})} \exp\left[- \sum_{j=1}^{J} \gamma_{ijr}^{*} y^{j} \right] \\ \psi(\gamma_{ir}^{*}) &= \int \exp\left[- \sum_{j=1}^{J} \gamma_{ijr}^{*} y^{j} \right] dy \end{aligned} \tag{5}$$

where the parameter vector γ_{ir}^{*} represents the solution to the maximization problem and $\psi(\gamma_{ir}^{*})$ is the normalizing factor that insures the density integrates to unity. The density in equation (5) is a member of the well-known exponential family.

Given the previously mentioned reasons for utilizing centered moments as constraints, we amend this framework slightly to utilize the mean, variance, and skewness of the yield distribution. The conditional variance and skewness are defined for each regime as

$$v_i^r \equiv E\left[(Y_i - \mu_{i1})^2 \mid \mathbf{X}_i = \mathbf{x}_i \right] = \mu_{i2}^r - (\mu_{i1}^r)^2, \tag{6}$$

$$s_i^r \equiv \frac{E\left[(Y_i - \mu_{i1})^3 \mid \mathbf{X}_i = \mathbf{x}_i \right]}{(v_i^r)^{3/2}} = \frac{\mu_{i3}^r - 3\mu_{i1}^r (\mu_{i1}^r)^2 + 2(\mu_{i1}^r)^3}{(v_i^r)^{3/2}}. \tag{7}$$

Using the conditional mean, variance, and skewness as the moment constraints, the new Lagrangian

is

$$\begin{aligned}\mathcal{L} &= -\int f(y)\ln f(y)\,dy - \gamma_0\left[\int f(y)\,dy - 1\right] - \gamma_1\left[\int y f(y)\,dy - \mu_{i1}^r\right] \\ &\quad -\gamma_2\left[\int (y-\mu_{i1}^r)^2 f(y)\,dy - v_i^r\right] - \gamma_3\left[\int \frac{(y-\mu_{i1}^r)^3}{(v_i^r)^{3/2}} f(y)\,dy - s_i^r\right]. \qquad (8)\end{aligned}$$

The implied maximum entropy density now takes the form

$$\begin{aligned}f_{ir}^*(y) &= \frac{1}{\psi(\gamma_{ir}^*)}\exp\left[-\gamma_{i1r}^* y - \gamma_{i2r}^*(y-\mu_{i1}^r)^2 - \gamma_{i3r}^*(y-\mu_{i1}^r)^3/(v_i^r)^{3/2}\right], \\ \psi(\gamma_{ir}^*) &= \int \exp\left[-\gamma_{i1r}^* y - \gamma_{i2r}^*(y-\mu_{i1}^r)^2 - \gamma_{i3r}^*(y-\mu_{i1}^r)^3/(v_i^r)^{3/2}\right] dy. \qquad (9)\end{aligned}$$

We use the maxentropy.ado file for Stata (Wittenberg, 2010) to estimate maximum entropy densities using the predicted conditional mean, variance, and skewness as constraints. The first step in constructing these constraints is to generate predicted raw moments using equation (1), which are then used to construct the conditional variance and skewness constraints according to equations (6) and (7). We estimate the maximum entropy distributions for every county-regime combination, thus allowing us to trace out spatially heterogeneous distributional effects of El Niño and La Niña.

3 Data

We combine three different data sources to construct a county-level panel of yield, temperature, precipitation, and ENSO data that spans 56 years. The limiting factor for this data is the temperature and precipitation data, which is only available from 1950-2005 and is discussed in more detail below.

County-level yield data are collected from the National Agricultural Statistics Service and are measured in bushels per acre. We include all counties that have a complete 56 year yield history, and further restrict our analysis to states that have at least five counties represented in the data. Table 1 provides a spatial representation of the data. There are a total of 55,384 observations representing 989 counties and 16 states. Six states are from the Western Corn Belt region, five

from the Eastern Corn belt, three from the Southeast, and one each from the East Coast and Mid South.

We use a monthly time series of the ENSO anomaly, *Niño 3.4*, derived from the index tabulated by the Climate Prediction Center at the National Oceanic and Atmospheric Administration. This index measures the difference in Sea Surface Temperature (SST) in the area of the Pacific Ocean between $5°N - 5°S$ and $170°W - 120°W$, and is a strong indicator of ENSO occurrence. The *Niño 3.4* monthly measure is an average of daily values interpolated from the weekly measures obtained both from satellites and actual locations around the Pacific. The anomaly is the deviation of the *Niño 3.4* monthly measure from the average historic measure for that particular month from the period 1971 – 2000.

In order to allow for El Niño and La Niña events to impact yields through vectors beyond temperature and precipitation, we utilize monthly SST anomaly data to construct dummy variables for each regime. For each year in the data set, we utilize the minimum and maximum monthly STT anomaly values (measured in $°C$) within the six month corn growing season (April through September) to construct the annual ranges shown in Figure 1. For each year, the top bar represents the highest monthly SST anomaly and the lower bar the lowest monthly anomaly. Denote by $\overline{sst_t}$ and $\underline{sst_t}$ the maximum and minimum of the six monthly measures in year t, then the El Niño and La Niña dummy variables are constructed according to

$$nino_t = \begin{cases} 1 \text{ if } \overline{sst_t} > 1°C \\ 0 \text{ otherwise} \end{cases} \qquad \text{and} \qquad nina_t = \begin{cases} 1 \text{ if } \underline{sst_t} < -1°C \\ 0 \text{ otherwise} \end{cases}$$

The above definition implies that any upper bar that breaks the $1°C$ line in Figure 1 denotes a growing season that was impacted by El Niño, and any lower bar that breaks the $-1°C$ line denotes a La Niña growing season. Thus, there are ten growing seasons that fall into the El Niño regime (1957, 1965, 1972, 1982, 1983, 1987, 1992, 1993, 1997, and 2002), and eleven that fall into the La Niña regime (1950, 1954, 1955, 1964, 1970, 1971, 1973, 1975, 1988, 1998, 1999). The remaining years thirty five years are considered the Neutral Regime.

Descriptive statistics for the data are reported in Table 2. The first set of statistics correspond

to the entire data, and the remaining sections correspond to the Neutral, El Niño, and La Niña regimes. We construct our yield measure as county-level production divided by harvested acres. Yields in the El Niño regime have a higher mean and lower variance compared to the Neutral regime, whereas yields in the La Niña regime have a lower mean and variance. However, yields across the regimes are not directly comparable because we have not taken into account the effect of technological change. Figure 2 provides box plots of the county-level yield data by year, and demonstrates that there is significant intra-annual variation across counties and a consistent increase in both the mean and variance of corn yields through time.

We use the same weather data as in Schlenker and Roberts (Schlenker and Roberts, 2009), which spans 1950-2005 and is based on the rectangular grid system underling PRISM that covers the contiguous United States. The authors construct a distribution of temperatures within each day using a sinusoidal curve between minimum and maximum temperatures. They then estimate time in each $1°C$ temperature interval between $-5°C$ and $50°C$. The area-weighted average time at each degree over all PRISM grid cells within a county is constructed, and are then summed over the six month corn growing season from April through September.

We use the same temperature intervals described in Schlenker and Roberts (Schlenker and Roberts, 2009). The measure of low temperature is constructed as the number of degree days above $0°C$ minus the number of degree days above $9°C$, thus capturing the number of degree days within the interval. The measure of medium temperature is constructed in the same way but with the bounds $10°C$ and $29°C$. The high measure is the number of degree days above $29°C$. Precipitation is measured in centimeters and is aggregated across the growing season in the same way as the temperature variables. Figure 3 provides annual box plots of the temperature and precipitation data.

Previous studies linking this weather data to yield outcomes (Tack et al., 2011; Schlenker and Roberts, 2006, 2009) have found that high temperatures and precipitation have a strong influence on yields. Table 2 shows that both the mean and variance of high temperatures under the El Niño and La Niña regimes increase relative to the neutral regime; thus suggesting periods of exposure to very extreme heat. This effect is much more pronounced for the La Niña regime in which both the

mean and variance increase substantially. For the precipitation variable, El Niño and La Niña have opposite effects. El Niño generates an increase in the mean and decrease in the variance, while La Niña generates a decrease in the mean and increase in the variance. Importantly, these measures are averages across several different regions of the U.S. which likely masks spatially heterogeneous effects of ENSO events on temperature and precipitation.

4 Results

The first subsection presents and discusses the results for the regression based estimation of the raw moments given by equation (1). The second subsection presents the maximum entropy distributions for the largest producing county within each state to demonstrate the qualitative effects of El Niño and La Niña on the shape of the corn yield distribution. In addition, the second subsection presents the quantitative effects of El Niño and La Niña on the mean and downside risk of the yield distribution for every county in the data.

4.1 Estimation of Raw Moments

Predicting the mean, variance, and skewness first requires estimating the first three raw moments according to the specifications given in equation (1). We estimate each equation and each state separately, and include county-level fixed effects and robust standard errors clustered at the county-level. There are over 3,000 parameters in the model, way too many to report here, so we will highlight the more interesting findings.

We find that the state-specific regression models for the three moments provide a reasonable level of fit for the data. Figure 4 provides the r-squared values of the three moment equations for each state. The goodness of fit statistic ranges from a low of 0.49 (Alabama, third moment) to a high of 0.90 (Minnesota, first moment). The range for the first moment equation is from 0.75 to 0.90, for the second it is from 0.61 to 0.84, and for the third it is from 0.49 to 0.76.

The left panel of Figure 5 reports 95 percent confidence intervals for the state-specific trend coefficients for the first moment equation. We find that technological change has had a positive and statistically significant effect on mean yields for all states. The non-overlap of the confidence

intervals provides evidence that there has been heterogeneous technological change across states. Although not reported, technological change continues to play an important causal role for the higher order moments. For the second and third moment equations, the linear trend variable is statistically significantly different from zero for all 16 states at a 1 percent significance level.

Recall that for equation j in state s, the overall effect of precipitation is given by $\beta_{js4} prec_{it} + \beta_{js5} prec_{it}^2$. To evaluate the causal role of precipitation, we conduct joint hypothesis tests of the form $H_0 : \beta_{js4} = \beta_{js5} = 0$. The right panel in Figure 5 reports the state-specific p-values associated with these tests for the first moment equation, and we find that the p-values are below 0.5 for all but two states. Although not reported here, the corresponding test results for the higher order moments imply that precipitation continues to play an important causal role for the higher order moments as the associated p-values are below 0.10 for 15 of the 16 states for both the second and third moment equations.

The left panel of Figure 6 reports 95 percent confidence intervals for the state-specific low temperature parameters for the first moment equation. We find that exposure to low temperature has a statistically significant effect on mean yields for 9 of the 16 states. Again, we see strong evidence of heterogeneity across states. Although not reported, exposure to low temperatures continues to play an important causal role for the higher order moments. For the second moment equation, the low temperature variable is statistically significantly different from zero for 11 states at a 10 percent significance level. The same finding exists for 12 states for the third moment equation.

The middle panel of Figure 6 reports 95 percent confidence intervals for the state-specific medium temperature parameters for the first moment equation. We find that exposure to medium temperature has a statistically significant effect on mean yields for 14 of the 16 states. Again, we see strong evidence of heterogeneity across states. Although not reported, exposure to medium temperatures continues to play an important causal role for the higher order moments. For the second moment equation, the medium temperature variable is statistically significantly different from zero for 14 states at a 5 percent significance level. The same finding exists for 15 states for the third moment equation.

The right panel of Figure 6 reports 95 percent confidence intervals for the state-specific low temperature parameters for the first moment equation. We find that exposure to high temperature has a negative and statistically significant effect on mean yields for all 16 states. Again, we see strong evidence of heterogeneity across states. Although not reported, exposure to high temperatures continues to play an important causal role for the higher order moments. For the second and third moment equations, the high temperature variable is statistically significantly different from zero for all 16 states at a 1 percent significance level.

The left panel of Figure 7 reports the state-specific parameter estimates and associated 95 percent confidence intervals of the El Niño dummy variable for the first moment equation. This approach allows us to test whether El Niño affects yields through vectors beyond temperature and precipitation, and we find that this is the case for 13 of the 16 states. Again, we see strong evidence of heterogeneity across states. Although not reported, the El Niño dummy variable continues to play an important causal role for the higher order moments. For the second and third moment equations, the El Niño variable is statistically significantly different from zero for 14 states at a 10 percent significance level.

The right panel of Figure 7 reports the state-specific parameter estimates and associated 95 percent confidence intervals of the La Niña dummy variable for the first moment equation. This approach allows us to test whether La Niña affects yields through vectors beyond temperature and precipitation, and we find that this is the case for all 16 states. Again, we see strong evidence of heterogeneity across states. Although not reported, the La Niña dummy variable continues to play an important causal role for the higher order moments. For the second moment equation, the La Niña variable is statistically significantly different from zero for 13 states at a 1 percent significance level. The same finding exists for 14 states for the third moment equation.

4.2 Mean and Downside Risk Effects

Following the procedure outlined in Empirical Framework section, we construct three maximum entropy distributions for each county, one for each ENSO regime. First, we use equation (1) and

the estimated parameters reported in the previous section to predict conditional moments as

$$\hat{\mu}_{ij}^{r} = \hat{\alpha}_{ij} + \hat{\beta}_{j}\bar{\mathbf{x}}_{i}^{r}, i = 1, \ldots, 969, j = 1, 2, 3, r \in \{nino, nina, neutral\}, \tag{10}$$

where $\bar{\mathbf{x}}_{i}^{r}$ are county-specific predictors under each regime. For the El Niño regime, we fix the temperature and precipitation variables at their sample average for the ten El Niño years, the El Niño and La Niña dummy variables are set to one and zero respectively, and we hold the trend variable at it sample average of twenty eight. We do the same for the La Niña regime using the eleven La Niña years, but fix the El Niño and La Niña variables to zero and one respectively. For the Neutral regime, we use the thirty five Neutral years to construct sample averages and fix both dummy variables to zero.

The next step is the construction of the conditional variance and skewness using the second and third moments from equation (10) combined with equations (6) – (7). This yields the final set of constraints for each county-regime combination, $\{\hat{\mu}_{i1}^{r}, \hat{v}_{i}^{r}, \hat{s}_{i}^{r}\}$, which are then used to estimate the maximum entropy density functions. Since we cannot report all of the estimated distributions here, we provide distributions for the largest producing county (based on historical average of production) within each state. These distributions are presented in Figures 8 – 10.

4.2.1 El Niño and La Niña Mean Effects

The effect of El Niño (La Niña) on mean corn yields is measured as the percentage change in the mean of the El Niño (La Niña) distribution relative to the mean of the Neutral distribution, i.e. $100 \times \left(\mu_{i}^{nino} - \mu_{i}^{neutral}\right)/\mu_{i}^{neutral}$ for El Niño and $100 \times \left(\mu_{i}^{nina} - \mu_{i}^{neutral}\right)/\mu_{i}^{neutral}$ for La Niña. Figure 11 reports state-specific box plots of the El Niño effect for all counties in the data. In the Western Corn Belt, the effect ranges from -13.3% to 7.8%, with 76 percent of all counties experiencing a reduction in yields. The range of effects in the Eastern Corn Belt is from -11.7% to 1.4 (96 percent), and in the Other Regions the range is -23.5% to 2.5% (97 percent). On average, the effect of El Niño is mean reducing, and there exists significant heterogeneity both within and across states. Interestingly, the largest reduction occurs in Maryland, and the average reduction in the Western and Eastern Corn Belts is small relative to the reductions in other regions.

Figure 12 reports state-specific box plots of the La Niña effect for all counties in the data. The effect ranges from −15.1% to 2.6% (97 percent experience a reduction) in the Western Corn Belt, from −13.0% to −1.3% (100 percent) in the Eastern Corn Belt, and from −24.1% to −4.4% (100 percent) for the Other Regions. The effect of La Niña is mean reducing for all but a few counties, and again we see strong evidence of spatial heterogeneity. On average, the effect is stronger as one moves eastward across the different regions with the largest reductions occurring in the Carolinas, Kentucky, and Maryland. Comparing the effects across figures 11 and 12, we see important asymmetries in the mean effects as the median effect in each state is typically larger under La Niña.

Figures 13 and 14 present spatial distributions of ENSO effects on mean corn yields across the U.S. These maps illustrate the asymmetries and heterogeneity of ENSO-related yield outcomes. La Niña events are the most damaging for the southern tier of both the Western and Eastern Corn Belt states, along with the Southeastern region of the U.S. Although, the magnitude of these effects are comparable (between 15 and 25 percent decrease in mean yield) the climatic reasons are different. In the case of the Corn Belt states this is because of excessive droughts, while in the case of the Southeastern states the likely reason for yield reductions are damaging storms associated with La Niña. Effects of El Niño are less severe but more heterogeneous. Most of the Corn Belt is only marginally affected by El Niño events, with an exception of central Iowa. Interestingly, negative El Niño effects are more dramatic in the neighborhood of the Appalachia.

Overall, our findings suggest that both El Niño and La Niña have a negative effect on mean corn yields for the majority of corn producing counties in our data, and that these effects are spatially heterogeneous both within and across the Western Corn Belt, Eastern Corn Belt, East, Southeast, and Mid South regions. These represent important findings as they conform with previously studies (Handler, 1990; Phillips et al., 1999; Jones, 1999) suggesting correlation between ENSO and corn yields in the Corn Belt and Southeastern region of the U.S. The findings suggest that the county-level analysis of ENSO effects is important, because the ENSO events may have diverging effects on corn yields in different parts of the same state.

4.2.2 El Niño and La Niña Downside Risk Effects

The effect of El Niño (La Niña) on downside risk is measured as the percentage change in the probability of a particular tail event under the El Niño (La Niña) distribution relative to the Neutral distribution. We define a catastrophic event in county i, Ω_i, as any outcome below sixty five percent of the mean of the Neutral Regime ($\hat{\mu}_{i1}^{neutral}$), i.e. $\Omega_i = \left\{y_i : y_i \leq 0.65\hat{\mu}_{i1}^{neutral}\right\}$. Define $y_i^* = 0.65\hat{\mu}_{i1}^{neutral}$ to be the threshold for the catastrophic event and denote by $F_{ir}(y)$ the cumulative distribution function associated with the maximum entropy distribution $f_{ir}(y)$, then the probability of a catastrophic event in any regime is just $F_{ir}(y_i^*)$. The effect of El Niño (La Niña) on a catastrophic event is measured as the percentage change in the probability under the El Niño (La Niña) distribution relative to the probability under the Neutral distribution, i.e. $100 \times \left[F_i^{nino}(y_i^*) - F_i^{neutral}(y_i^*)\right] / F_i^{neutral}(y_i^*)$ for El Niño, and $100 \times \left[F_i^{nina}(y_i^*) - F_i^{neutral}(y_i^*)\right] / F_i^{neutral}(y_i^*)$ for La Niña.

Figure 15 reports state-specific box plots of the El Niño downside risk effect for all counties in the data. The effect ranges from -79.0% to 42.3% (72 percent experience a reduction) in the Western Corn Belt, from -67.9% to 48.8% (71 percent) in the Eastern Corn Belt, and from -99.1% to 90.8% (51 percent) in the Other Regions. It is evident that El Niño can be both risk reducing and risk enhancing, and that this heterogeneity occurs both within and across most states.

Figure 16 reports state-specific box-plots of the La Niña downside risk effect. The effect ranges from -47.6% to 66.1% (2 percent experience a reduction) in the Western Corn Belt, from -16.6% to 143.9% (less than 1 percent) in the Eastern Corn Belt, and from -63.3% to 79.5% (9 percent) in the Other Regions. Alternative to the El Niño findings, these results suggest La Niña events are associated with an increase in downside risk, and that these increases can be quite large. On average, the largest effects occur in Illinois and Wisconsin, and the Eastern Corn Belt as a whole experiences larger increases relative to other parts of the U.S.

Spatial distributions of these effects are illustrated in Figures 17 and 18. El Niño effects prove to be heterogeneous across different regions of the U.S. In central Iowa, as well as western parts if Illinois and Ohio, El Niño results in up to a 40 percent increase in the probability of a catastrophic event. On the contrary, in South Dakota, Nebraska and Missouri, as well as the Mid South and the Southeastern regions of the U.S. the probabilities of catastrophic events decrease during El Niño.

Reasons for this could be low probabilities of droughts in the Midwest, as well as mitigation of damaging storm and hurricanes in the Southeastern region during an El Niño event. Alternatively, La Niña consistently increases probabilities of catastrophic events across the corn producing regions. The largest relative changes in downside risk are observed in the heart of the Corn Belt, most likely due to exacerbated drought conditions. Finally, the sign and magnitude of the La Niña effect on downside risk is respectively less consistent and smaller in the Southeastern U.S.

Overall, our findings suggest that La Niña has a negative effect on downside risk for the majority of corn producing counties in our data, while the El Niño effects are spatially heterogeneous both within and across the U.S. These represent important findings as they provide additional insights about ENSO's impact on corn production, and represent a useful aid for downside risk management for both crop producers and government agencies.

5 Conclusions

ENSO's impact on world commodity production and prices has well been documented, and recent research suggests a causal relationship with social unrest and civil conflict (e.g. Handler, 1990; Solow et al., 1998; Brunner, 2002; Ubilava and Holt, 2009; Hsiang et al., 2011). However, research focused on higher order effects of ENSO is lacking, especially in the area of agricultural production. This is the focus of this article, as we illustrate the impacts of ENSO on U.S. corn production using county-level data spanning 1950 to 2005. Our findings greatly complement previous studies and have implications for researchers and policy makers in several disciplines including production, climate change, and civil unrest.

Our findings have strong implications for modelling efforts linking ENSO events to agricultural production. Previous approaches primarily focus on the effects of ENSO on the mean of the yield distribution, rather than the distribution itself. This approach is short sighted as our findings clearly demonstrate that ENSO events can dramatically alter probabilities of large scale crop losses. We remedy this short-coming of current modeling approaches by providing an empirical framework that is tractable, utilizes actual yield history that is publicly available, and is not restrictive in the number of locations included. This approach has several advantages over simulation-based exercises

as in Legler, Bryant, and O'brien and Chen, McCarl, and Adams (Legler et al., 1999; Chen et al., 2001). Within this framework, we also demonstrate how the effect of ENSO on crop yields can be modeled through multiple causal vectors in a regression based framework, rather than adopting *ad hoc* methods that estimate the effect through groupings of regression residuals (Chen et al., 2008) or the use of spectral density methods (Hansen et al., 1998).

This study has immediate implications for corn producers and policy makers as our results clearly demonstrate that ENSO events alter the entire distribution of yields. Interestingly, these effects are asymmetric across the two major ENSO events, El Niño and La Niña, and spatially heterogeneous. While we focus on U.S. corn yields, it is likely that these findings extend to other crops and countries. We demonstrate ENSO's effect on downside risk, which represents a key finding for risk management decision making and development of agricultural policy instruments. An interesting line of future research would be to combine the conditional yield distributions derived in this article with a predictive model of ENSO events to formulate *ex ante* unconditional yield distributions. To the extent that these unconditional distributions differ from current approaches that ignore ENSO impacts, this line of research would help producers better manage their exposure to risk and help policy makers construct more efficient policy instruments.

The nexus of climate change and agricultural production research continues to focus on the mean of the yield distribution, and assumes that the key predictive variables are temperature and precipitation. These approaches omit the impacts of ENSO events under future climate scenarios, even though evidence suggests that ENSO events and climate change are correlated. We demonstrate that temperature and precipitation are not the only vectors by which ENSO affects yields, thus implying that the omission of variables that control for ENSO events in a predictive yield model is likely problematic.

There exists a burgeoning scientific literature linking climatic phenomenons to civil unrest in developing countries where food shortages and poverty are consistent concerns (Hsiang et al., 2011). The exact mechanism by which ENSO causes social unrest has not been credibly identified, however high commodity prices have been linked to social unrest (Barrett and Bellemare, 2011; Bellemare, 2011). We find evidence that ENSO events, particularly La Niña, can generate large increases in

the probability of catastrophic crop losses. Given that these increased probabilities occur for nearly all of the counties in our data, realized crop losses could occur simultaneously across large, diverse production regions . This is exactly the type of outcome that could trigger large price spikes and consequently civil unrest. Thus, our findings contribute to this literature by providing a candidate for the missing piece in the causal chain linking ENSO events to civil unrest.

References

Adams, R., C. Chen, B. McCarl, and R. Weiher (1999). The Economic Consequences of ENSO Events for Agriculture. *Climate Research 13*(3), 165–172.

Antle, J. (2010). Asymmetry, Partial Moments and Production Risk. *American Journal of Agricultural Economics 92*(5), 1294–1309.

Barlow, M., S. Nigam, and E. Berbery (2001). ENSO, Pacific Decadal Variability, and US Summertime Precipitation, Drought, and Stream Flow. *Journal of Climate 14*(9), 2105–2128.

Barrett, C. and M. Bellemare (2011, July). Why Food Price Volatility Doesn't Matter. Foreign Affairs.

Bellemare, M. (2011). Rising Food Prices, Food Price Volatility, and Political Unrest. Working Paper.

Bove, M., , J. Eisner, C. Landsea, X. Niu, and J. O'Brien (1998). Effect of El Niño on U.S. Landfalling Hurricanes, Revisited. *Bulletin of the American Meteorological Society 79*(11), 2477–2482.

Brenner, J. (1991). Southern Oscillation Anomalies and their Relationship to Wildfire Activity in Florida. *International Journal of Wildland Fire 1*(1), 73–78.

Brunner, A. (2002). El Nino and World Primary Commodity Prices: Warm Water or Hot Air? *Review of Economics and Statistics 84*(1), 176–183.

Carlson, R., D. Todey, and S. Taylor (1996). Midwestern Corn Yield and Weather in Relation to Extremes of the Southern Oscillation. *Journal of Production Agriculture 9*(3), 347–352.

Chavas, J. and M. Holt (1996). Economic Behavior under Uncertainty: A Joint Analysis of Risk Preferences and Technology. *Review of Economics and Statistics 78*(2), 329–335.

Chen, C., B. McCarl, and R. Adams (2001). Economic Implications of Potential ENSO Frequency and Strength Shifts. *Climatic Change 49*(1), 147–159.

Chen, C., B. McCarl, and C. Chang (2008). Strong El Nino-Southern Oscillation Events and the Economics of the International Rice Market. *Climate Research 36*(2), 113.

Chen, C., B. McCarl, and H. Hill (2002). Agricultural Value of ENSO Information under Alternative Phase Definition. *Climatic Change 54*(3), 305–325.

Chen, C., B. McCarl, and D. Schimmelpfennig (2004). Yield Variability as Influenced by Climate: A Statistical Investigation. *Climatic Change 66*(1), 239–261.

Dalton, M. (2001). El Niño, Expectations, and Fishing Effort in Monterey Bay, California. *Journal of Environmental Economics and Management 42*(3), 336–359.

Day, R. (1965). Probability distributions of field crop yields. *Journal of Farm Economics 47*(3), 713.

Eltahir, E. (1996). El Niño and the Natural Variability in the Flow of the Nile River. *Water Resources Research 32*(1), 131–137.

Gallagher, P. (1987). Us soybean yields: Estimation and forecasting with nonsymmetric disturbances. *American Journal of Agricultural Economics 69*(4), 796.

Goodwin, B. and A. Ker (1998). Nonparametric estimation of crop yield distributions: Implications for rating group-risk crop insurance contracts. *American Journal of Agricultural Economics 80*(1), 139.

Hall, A., J. Skalin, and T. Teräsvirta (2001). A Nonlinear Time Series Model of El Niño. *Environmental Modelling & Software 16*(2), 139–146.

Handler, P. (1984). Corn Yields in the United States and Sea Surface Temperature Anomalies in the Equatorial Pacific Ocean During the Period 1868–1982. *Agricultural and Forest Meteorology 31*(1), 25–32.

Handler, P. (1990). USA Corn Yields, The El Niño and Agricultural Drought: 1867–1988. *International Journal of Climatology 10*(8), 819–828.

Handler, P. and E. Handler (1983). Climatic Anomalies in the Tropical Pacific Ocean and Corn Yields in the United States. *Science 220*(4602), 1155–1156.

Hansen, J., A. Hodges, and J. Jones (1998). ENSO Influences on Agriculture in the Southeastern United States. *Journal of Climate 11*(3), 404–411.

Haug, G., D. Gunther, L. Peterson, D. Sigman, K. Hughen, and B. Aeschlimann (2003). Climate and Tthe Collapse of Mayan Civilization. *Science 299*, 1731–35.

Hennessy, D. (2009a). Crop Yield Skewness and the Normal Distribution. *Journal of Agricultural and Resource Economics 34*(1), 34–52.

Hennessy, D. (2009b). Crop Yield Skewness Under Law of the Minimum Technology. *American Journal of Agricultural Economics 91*(1), 197.

Hsiang, S., K. Meng, and M. Cane (2011). Civil Conflicts are Associated with the Global Climate. *Nature 476*, 438–441.

Iglesias, A. and C. Rosenzweig (2007). Climate and Pest Outbreaks. *Encyclopedia of Pest Management 2*, 87.

Jones, J. (1999). Atlantic and Pacific Sea Surface Temperatures and Corn Yields in the Southeastern USA: Lagged Relationships and Forecast Model Development. *International Journal of Climatology 31*(4), 592–604.

Kelly, D., C. Kolstad, and G. Mitchell (2005). Adjustment Costs from Environmental Change. *Journal of Environmental Economics and Management 50*(3), 468–495.

Ker, A. and K. Coble (2003). Modeling conditional yield densities. *American Journal of Agricultural Economics 85*(2), 291.

Kiladis, G. and H. Diaz (1989). Global Climatic Anomalies Associated with Extremes in the Southern Oscillation. *Journal of Climate 2*(9), 1069–1090.

Kim, M. and B. McCarl (2005). The Agricultural Value of Information on the North Atlantic Oscillation: Yield and Economic Effects. *Climatic Change 71*(1), 117–139.

Legler, D., K. Bryant, and J. O'Brien (1999). Impact of ENSO-related Climate Anomalies on Crop Yields in the U.S. *Climatic Change 42*(2), 351–375.

Montroy, D. (1997). Linear Relation of Central and Eastern North American Precipitation to Tropical Pacific Sea Surface Temperature Anomalies. *Journal of Climate 10*(4), 541–558.

Moschini, G. and D. Hennessy (2001). Uncertainty, Risk Aversion, and Risk Management for Agricultural Producers. *Handbook of Agricultural Economics 1*, 88–153.

Moss, C. and J. Shonkwiler (1993). Estimating yield distributions with a stochastic trend and nonnormal errors. *American Journal of Agricultural Economics 75*(4), 1056.

Nelson, C. and P. Preckel (1989). The conditional beta distribution as a stochastic production function. *American Journal of Agricultural Economics 71*(2), 370.

Noel, J. and D. Changnon (1998). A Pilot Study Examining U.S. Winter Cyclone Frequency Patterns Associated with Three ENSO Parameters. *Journal of Climate 11*(8), 2152–2159.

Phillips, J., B. Rajagopalan, M. Cane, and C. Rosenzweig (1999). The Role of ENSO in Determining Climate and Maize Yield Variability in the U.S. Cornbelt. *International Journal of Climatology 19*(8), 877–888.

Ramirez, O., S. Misra, and J. Field (2003). Crop-yield distributions revisited. *American Journal of Agricultural Economics 85*(1), 108.

Rasmusson, E. (1991). *Teleconnections Linking Worldwide Climate Anomalies*, Chapter Observational Aspects of ENSO Cycle Teleconnections, pp. 309–343. Cambridge University Press, New York.

Ropelewski, C. and M. Halpert (1986). North American Precipitation and Temperature Patterns Associated with the El Niño/Southern Oscillation (ENSO). *Monthly Weather Review 114*(12), 2352–2362.

Ropelewski, C. and M. Halpert (1987). Global and Regional Scale Precipitation Patterns Associated with the El Niño/Southern Oscillation. *Monthly Weather Review 115*(8), 1606–1626.

Rosenzweig, C., A. Iglesias, X. Yang, P. Epstein, and E. Chivian (2000). Climate Change and U.S. Agriculture: The Impacts of Warming and Extreme Weather Events on Productivity, Plant Diseases, and Pests. Center for Health and the Global Environment, Harvard Medical School, Boston, MA, USA.

Saunders, M., R. Chandler, C. Merchant, and F. Roberts (2000). Atlantic Hurricanes and NW Pacific Typhoons: ENSO Spatial Impacts on Occurrence and Landfall. *Geophysical research letters 27*(8), 1147–1150.

Schlenker, W. and M. Roberts (2006). Nonlinear Effects of Weather on Corn Yields. *Applied Economic Perspectives and Policy 28*(3), 391.

Schlenker, W. and M. Roberts (2009). Nonlinear Temperature Effects Indicate Severe Damages to US Crop Yields under Climate Change. *Proceedings of the National Academy of Sciences 106*(37), 15594.

Sherrick, B., F. Zanini, G. Schnitkey, and S. Irwin (2004). Crop insurance valuation under alternative yield distributions. *American Journal of Agricultural Economics 86*(2), 406.

Shohat, J. and J. Tamarkin (1943). *The Problem of Moments*, Volume 1. American Mathematical Society.

Solow, A., R. Adams, K. Bryant, D. Legler, J. O'Brien, B. McCarl, W. Nayda, and R. Weiher (1998). The Value of Improved ENSO Prediction to US Agriculture. *Climatic Change 39*(1), 47–60.

Stohs, S. (2003). *A Bayesian Updating Approach to Crop Insurance Ratemaking*. Ph. D. thesis, University of California – Berkeley.

Stone, R., G. Hammer, and T. Marcussen (1996). Prediction of Global Rainfall Probabilities Using Phases of the Southern Oscillation Index. *Nature 384*, 252–255.

Swetnam, T. and J. Betancourt (1990). Fire–Southern Oscillation Relations in the Southwestern United States. *Science 249*(4972), 1017.

Tack, J., A. Harri, and K. Coble (2011). More than Mean Effects: Modeling the Effect of Climate on the Higher Order Moments of Crop Yields. SSRN eLibrary. Working Paper Series.

Timmermann, A., J. Oberhuber, A. Bacher, M. Esch, M. Latif, and E. Roeckner (1999). Increased El Niño Frequency in a Climate Model Forced by Future Greenhouse Warming. *Nature 398*, 694–697.

Tsonis, A., K. Swanson, G. Sugihara, and P. Tsonis (2010). Climate Change and the Demise of Minoan Civilization. *Climate of the Past Discussions 6*, 801–815.

Ubilava, D. and M. Holt (2009). Nonlinearities in the world vegetable oil price system: El nino effects. In *2009 Annual Meeting, July 26-28, 2009, Milwaukee, Wisconsin*. Agricultural and Applied Economics Association.

Wittenberg, M. (2010). An introduction to maximum entropy and minimum cross-entropy estimation using stata. *Stata Journal 10*(3), 315–330.

Tables

Table 1: Spatial Representation of Data

State	Number Counties	Obs
Western Corn Belt		
Iowa	99	5,544
Minnesota	58	3,248
Missouri	83	4,648
Nebraska	89	4,984
North Dakota	14	784
South Dakota	53	2,968
Eastern Corn Belt		
Illinois	102	5,712
Indiana	87	4,872
Michigan	42	2,352
Ohio	82	4,592
Wisconsin	58	3,248
Southeast		
Alabama	17	952
North Carolina	73	4,088
South Carolina	30	1,680
East Cost		
Maryland	21	1,176
Mid South		
Kentucky	81	4,536
United States		
Total	989	55,384

Notes: We only include counties that have a complete yield histroy from 1950-2005.

Table 2: Yield and Climate Data: 1950-2005

Variable	Sample Mean	(s.d.)	Min	Max	Obs
All Years					
Corn Yield (bushels per acre)	85.36	(36.56)	0.04	200.00	55384
Low Temperature (degree days)	2445.50	(140.57)	1425.70	1829.40	55384
Medium Temperature (degree days)	1009.50	(249.14)	848.30	2703.40	55384
High Temperature (degree days)	25.94	(24.16)	0.00	240.43	55384
Precipitation (centimeters)	56.87	(14.61)	11.76	147.19	55384
El Nino (Yes = 1)	0.18	(0.38)	0.00	1.00	55384
La Nina (Yes = 1)	0.20	(0.40)	0.00	1.00	55384
Neutral Regime					
Corn Yield (bushels per acre)	87.29	(37.10)	4.00	200.00	34615
Low Temperature (degree days)	1720.20	(65.04)	1460.31	1828.21	34615
Medium Temperature (degree days)	1728.60	(317.62)	928.88	2694.61	34615
High Temperature (degree days)	24.21	(22.73)	0.00	216.85	34615
Precipitation (centimeters)	56.66	(14.48)	11.76	132.13	34615
El Niño Regime					
Corn Yield (bushels per acre)	92.45	(33.69)	10.00	195.28	9890
Low Temperature (degree days)	1708.70	(67.75)	1458.62	1828.11	9890
Medium Temperature (degree days)	1708.40	(337.87)	848.31	2663.25	9890
High Temperature (degree days)	24.60	(23.48)	0.01	139.85	9890
Precipitation (centimeters)	59.00	(14.38)	17.00	126.93	9890
La Niña Regime					
Corn Yield (bushels per acre)	72.80	(34.35)	0.04	172.39	10879
Low Temperature (degree days)	1726.50	(66.13)	1425.77	1829.43	10879
Medium Temperature (degree days)	1782.50	(313.44)	922.39	2703.47	10879
High Temperature (degree days)	32.64	(27.75)	0.05	240.43	10879
Precipitation (centimeters)	55.57	(15.04)	16.17	147.20	10879

Notes: Values reported for temperature and precipitation variables correspond to the April through September growing season. Low temperature measures degree days between $0°C$ and $9°C$; medium temperature measures degree days between $10°C$ and $29°C$; and high temperature measures degree days above $29°C$. A list of the El Niño, La Niña, and Neutral years is provided in the text.

Figures

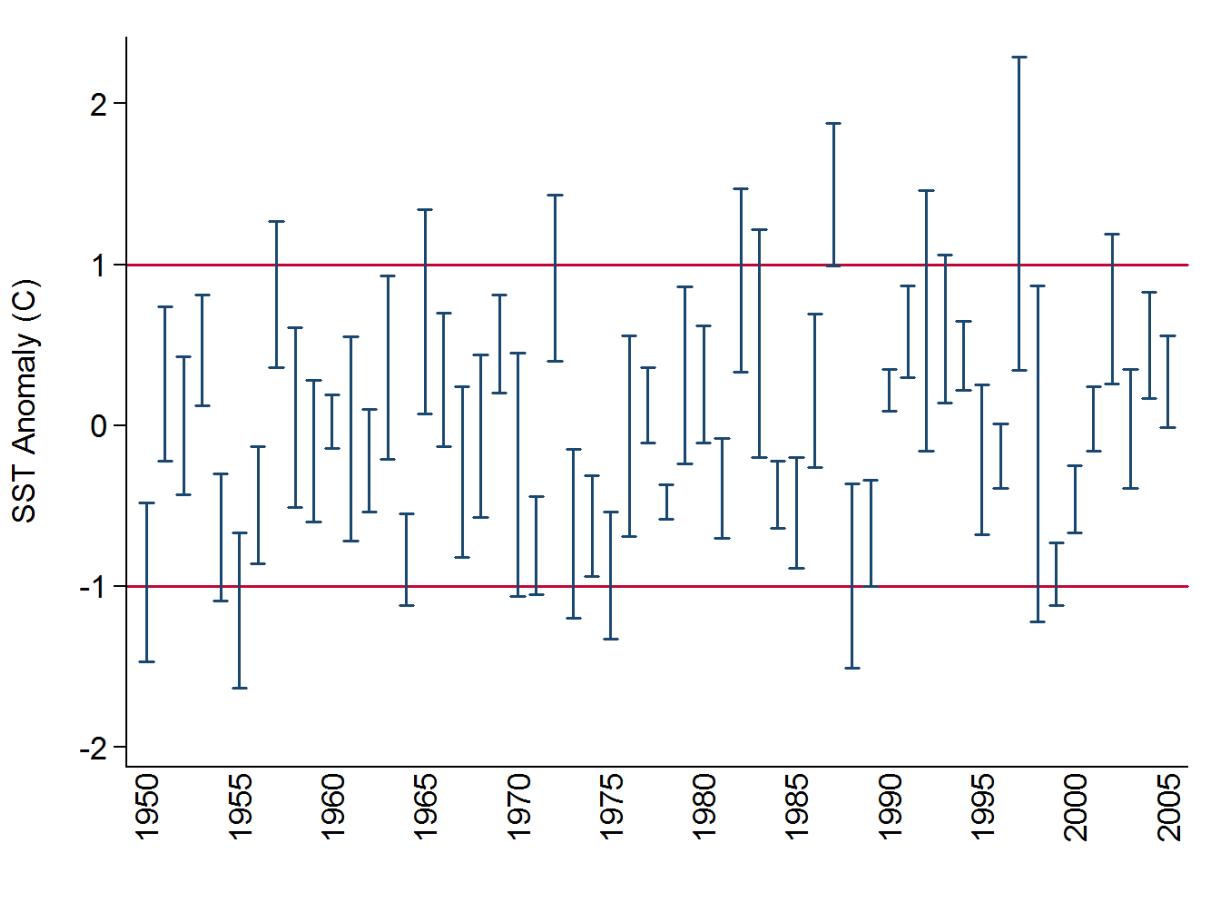

Figure 1: SST Anomalies During the Growing Seasons

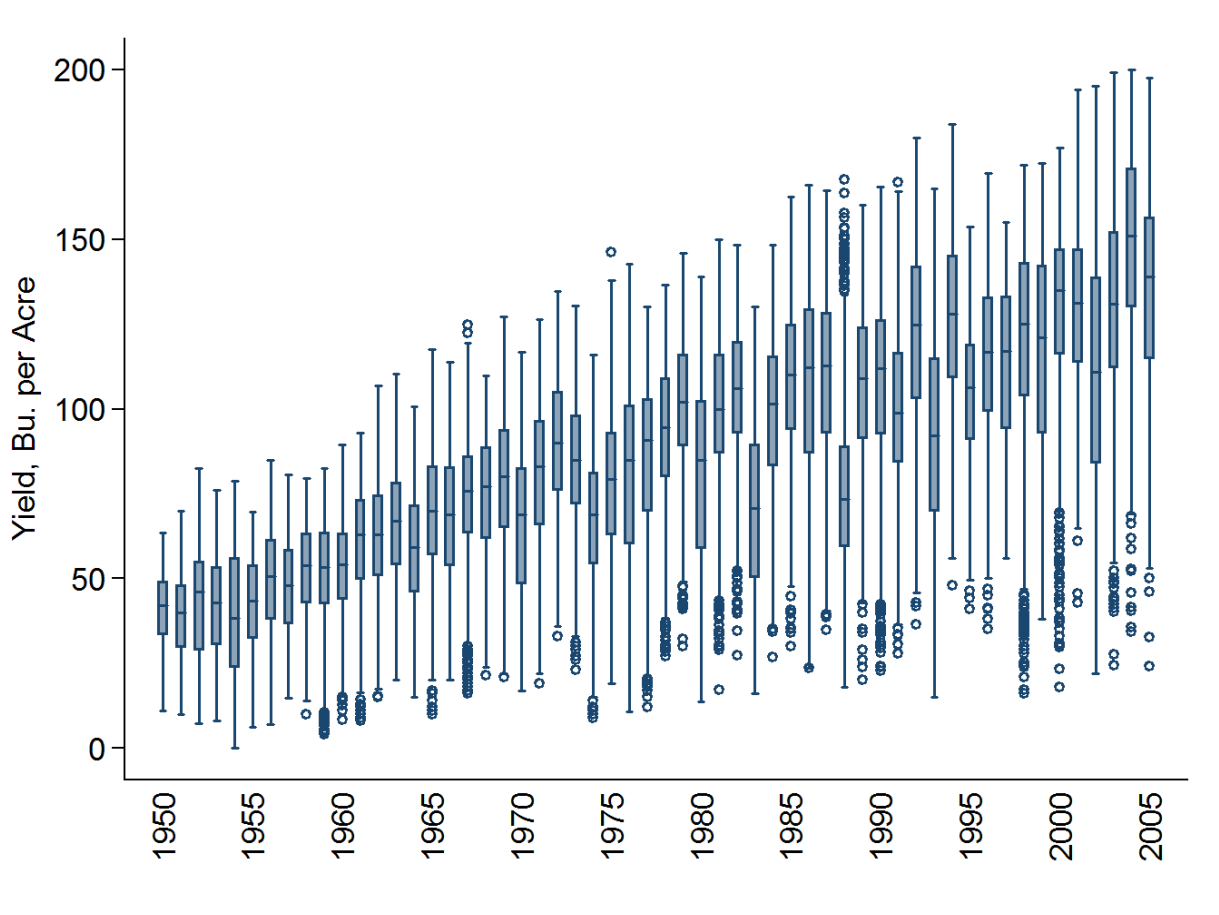

Figure 2: Corn Yields across Counties by Year

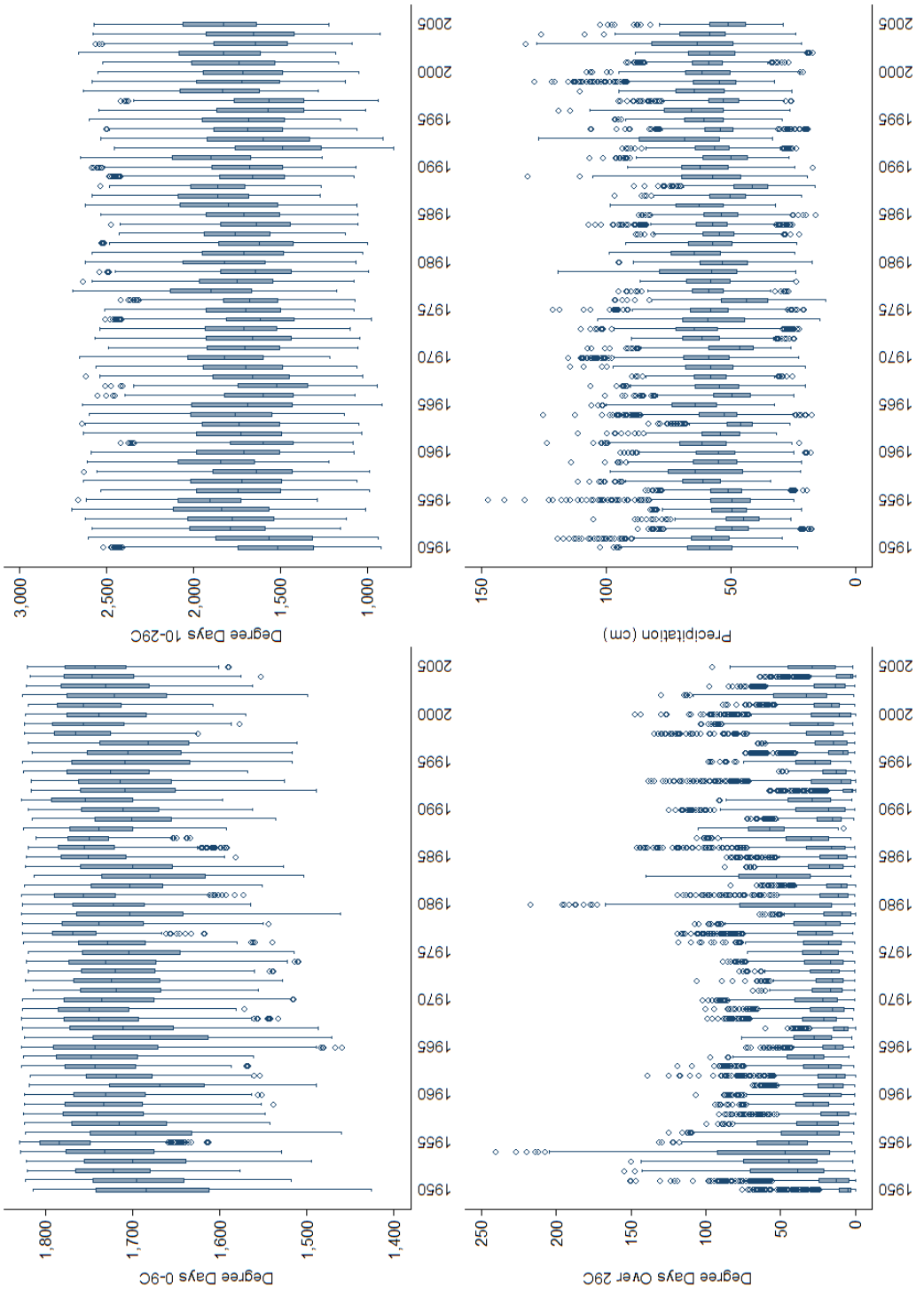

Figure 3: Temperature and Precipitation Across Counties by Year

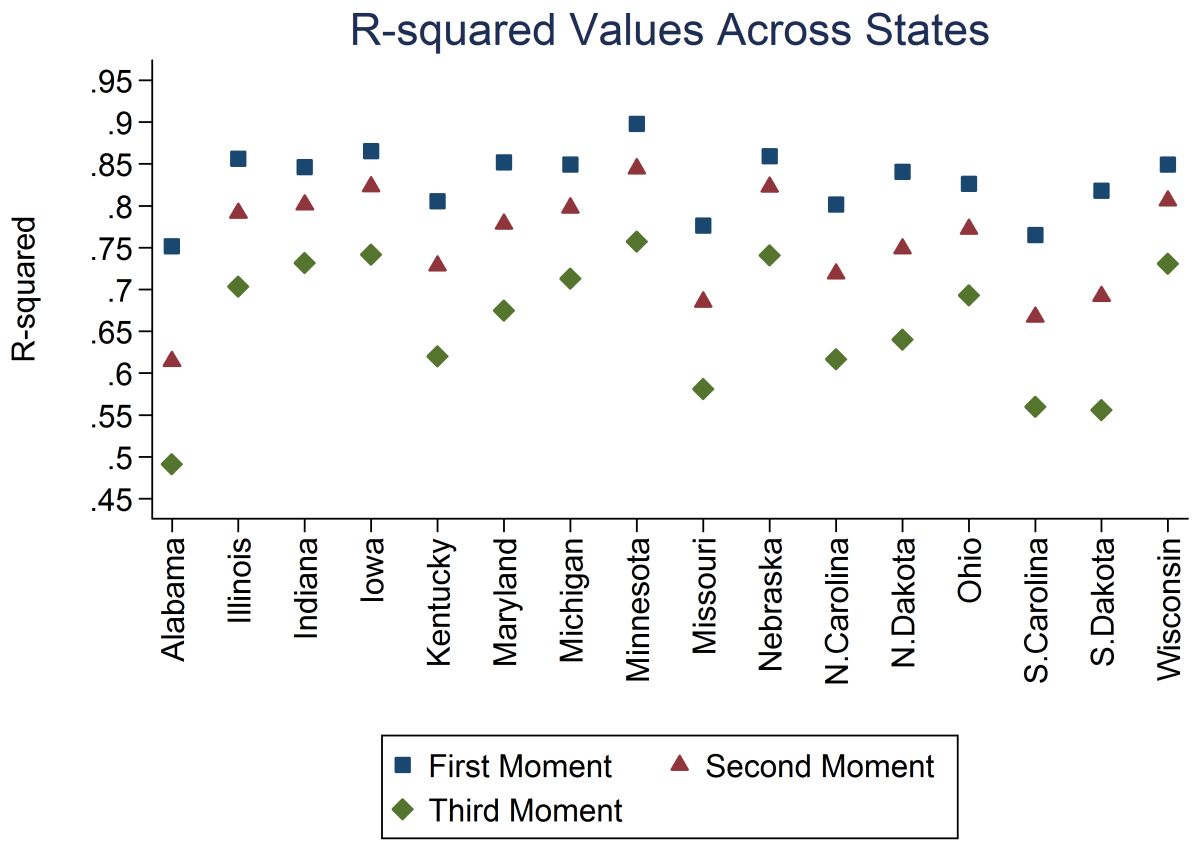

Figure 4: R^2 Values of the Three Moments Equations by State

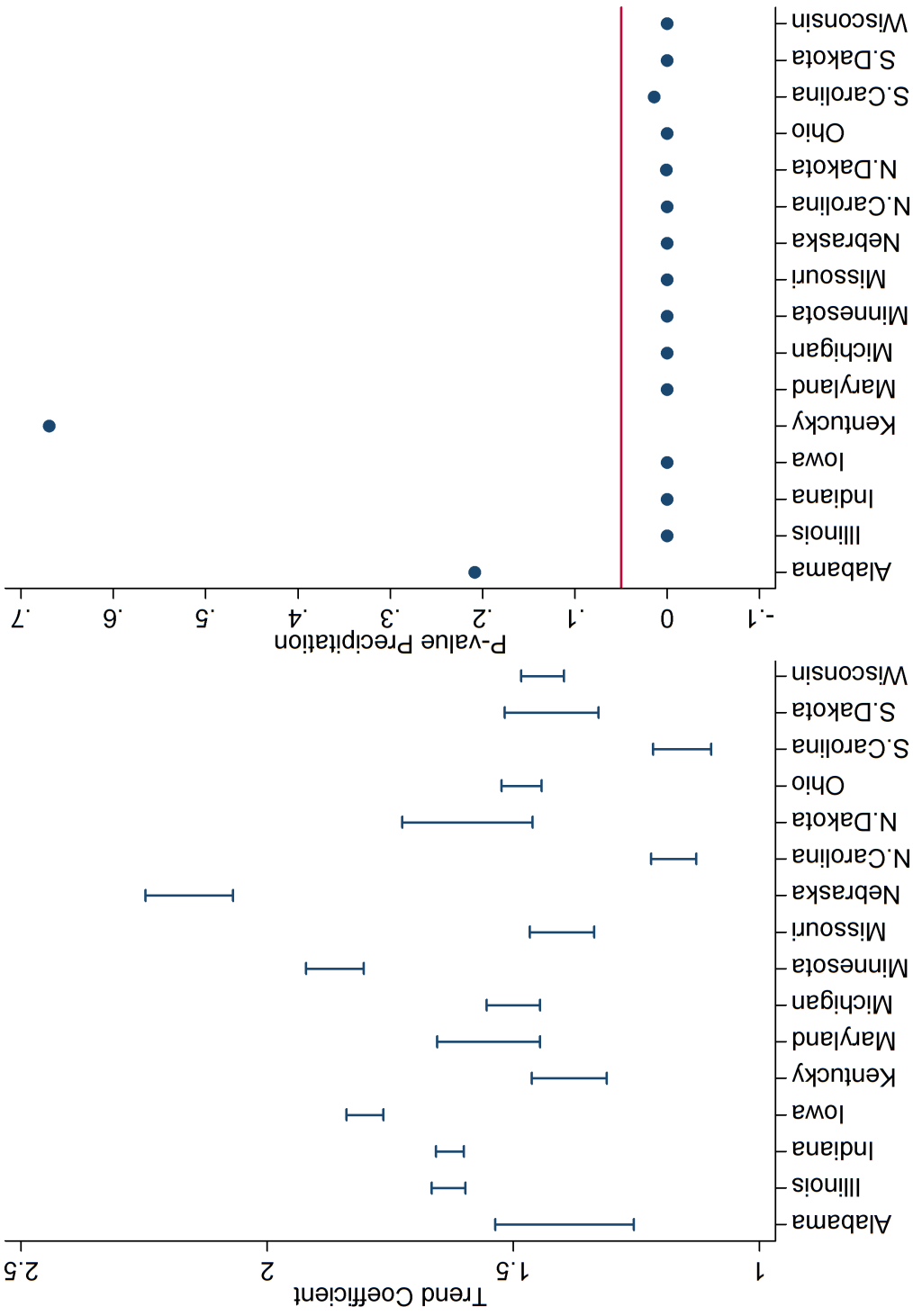

Figure 5: Statistical Significance of Technological Change and Precipitation Parameters by State

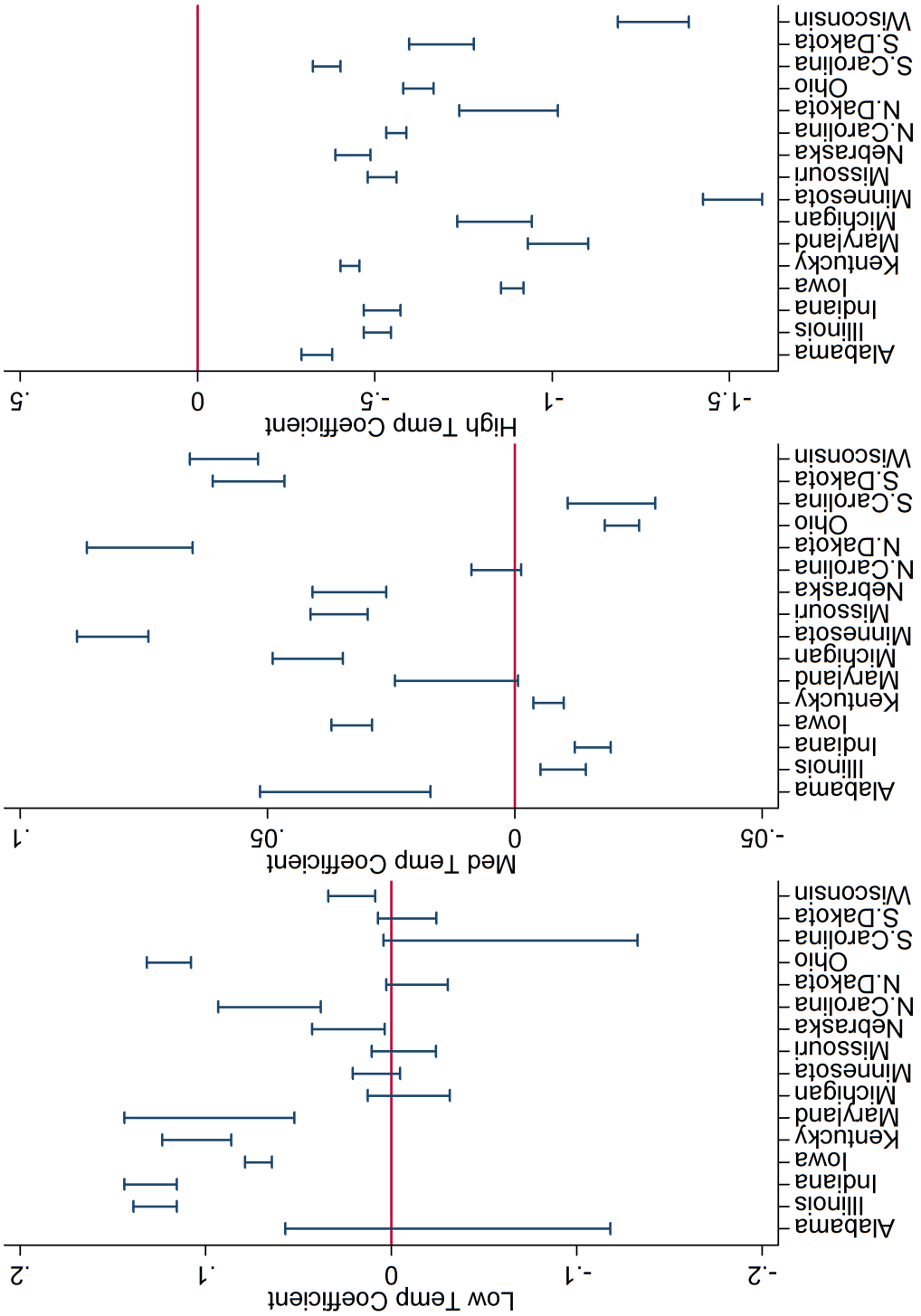

Figure 6: Low, Medium and High Temperature Parameters by State

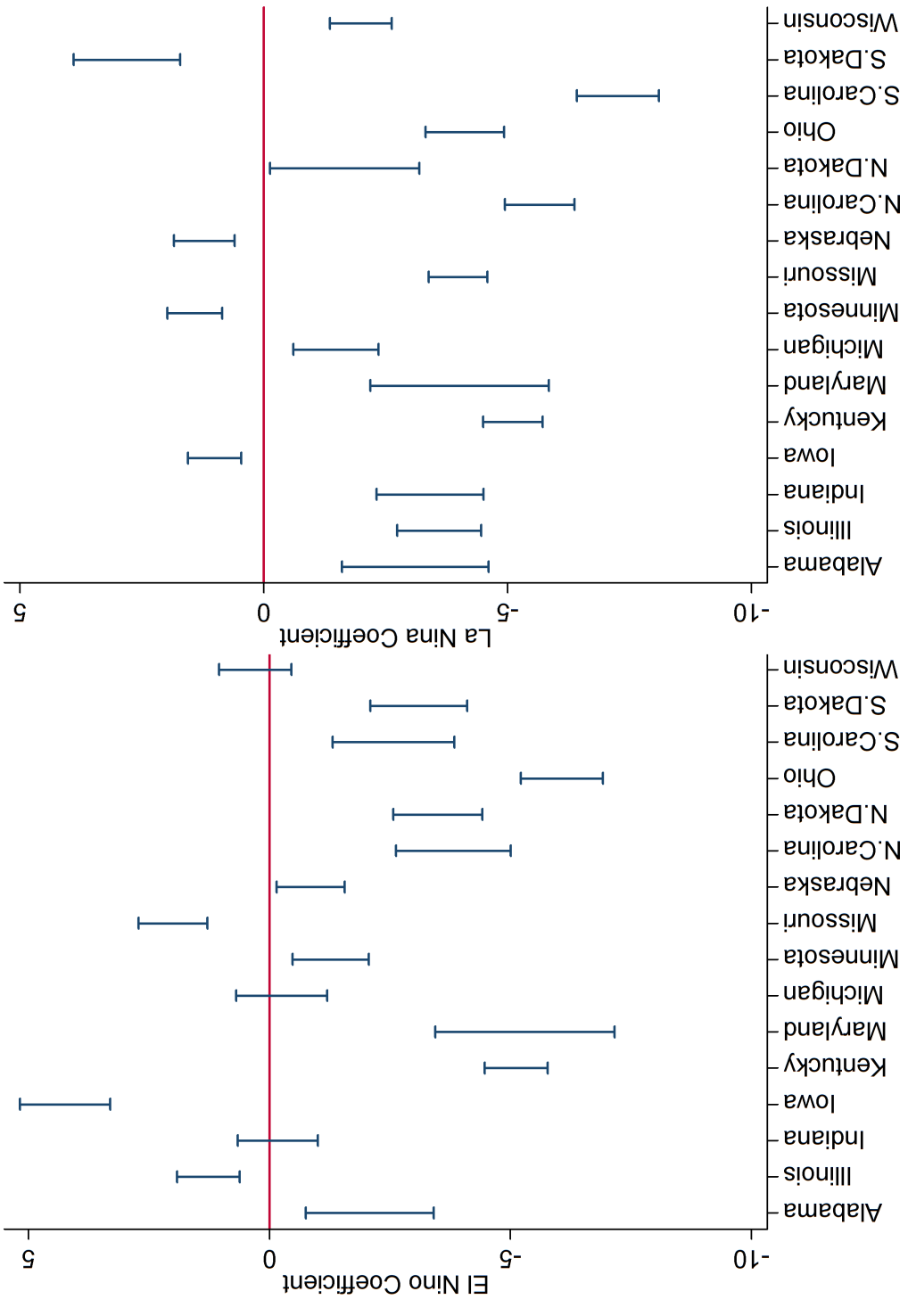

Figure 7: El Niño and La Niña Parameters by State

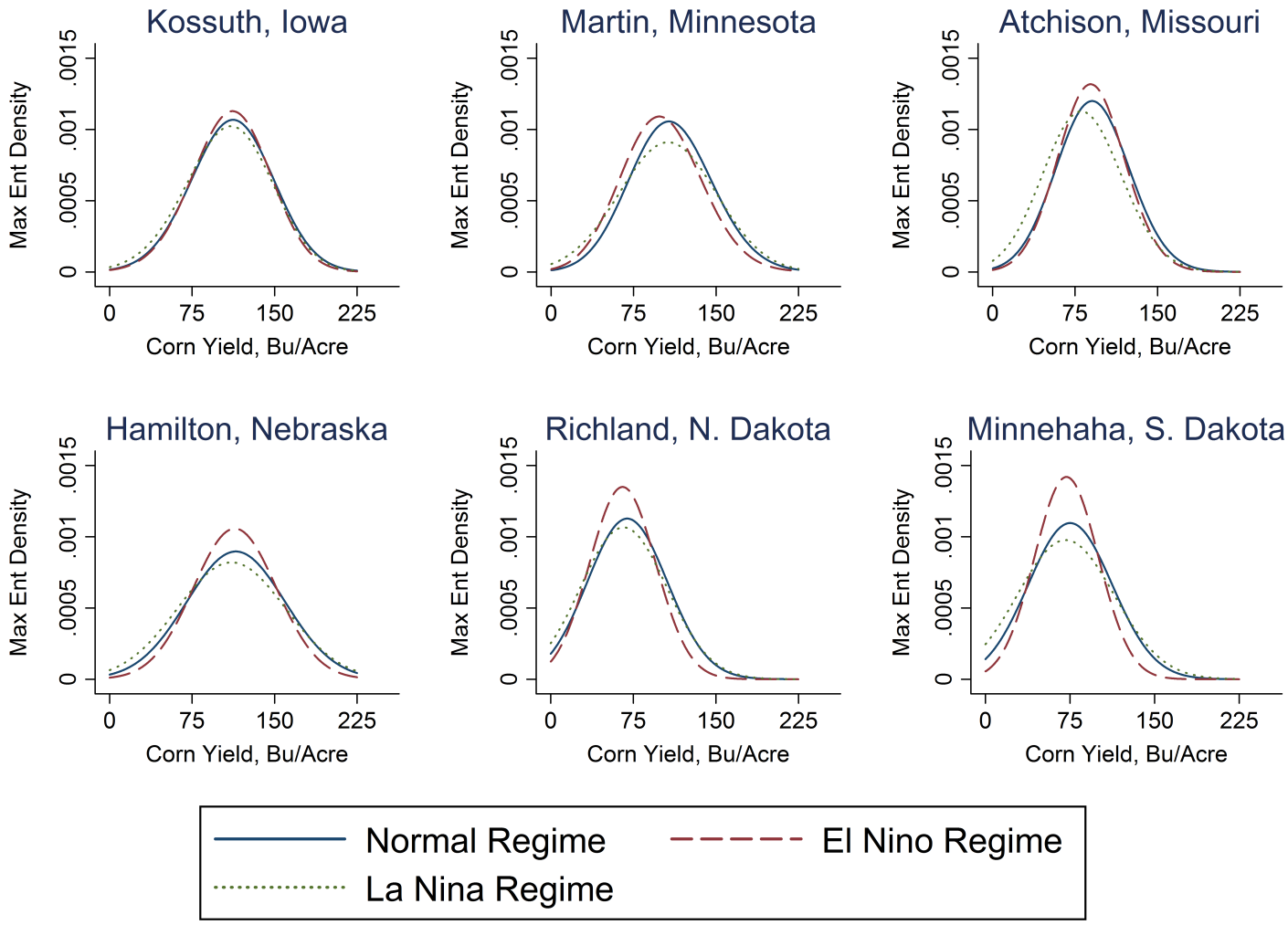

Figure 8: Yield Distributions in the Western Corn Belt Region

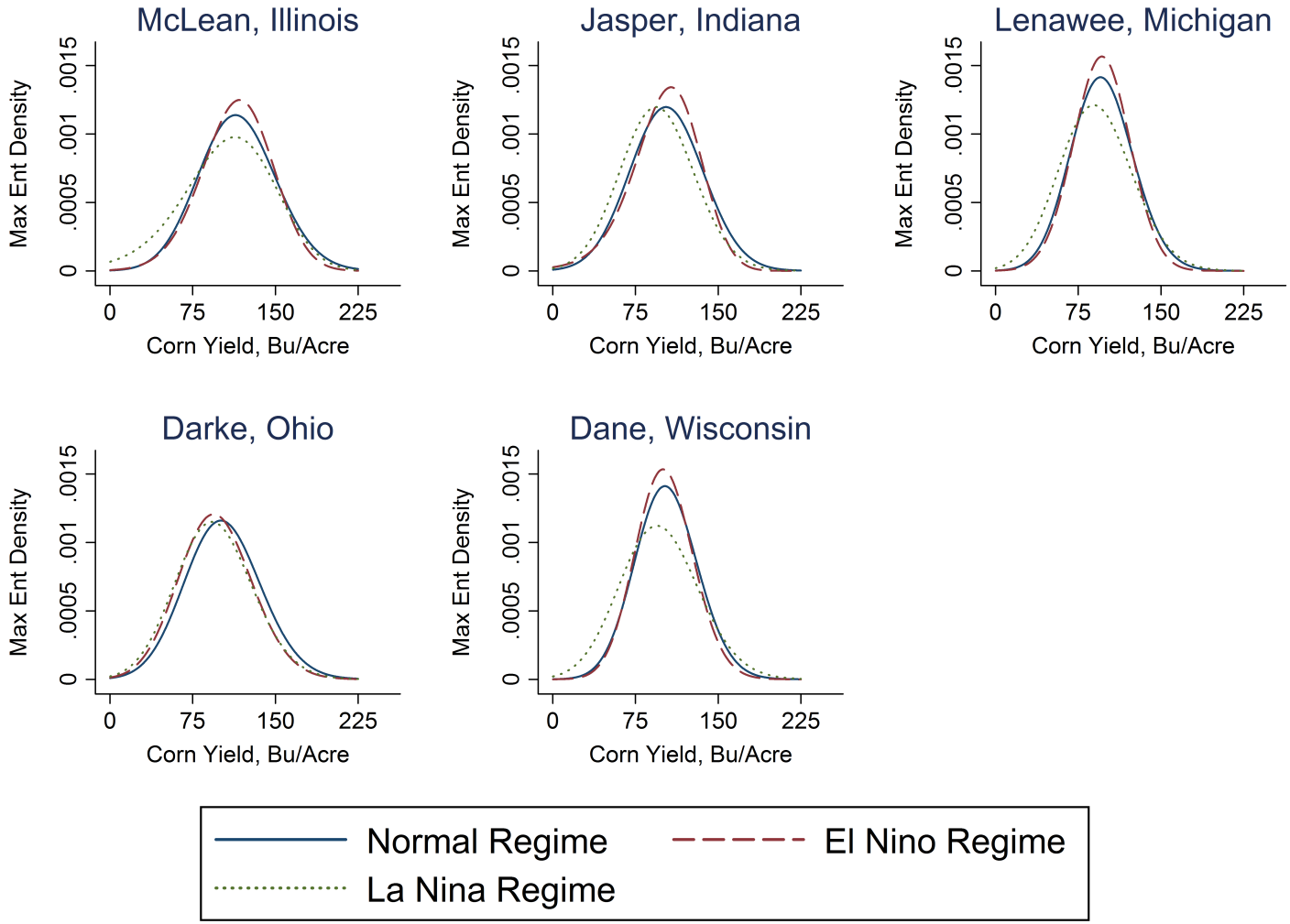

Figure 9: Yield Distributions in the Eastern Corn Belt Region

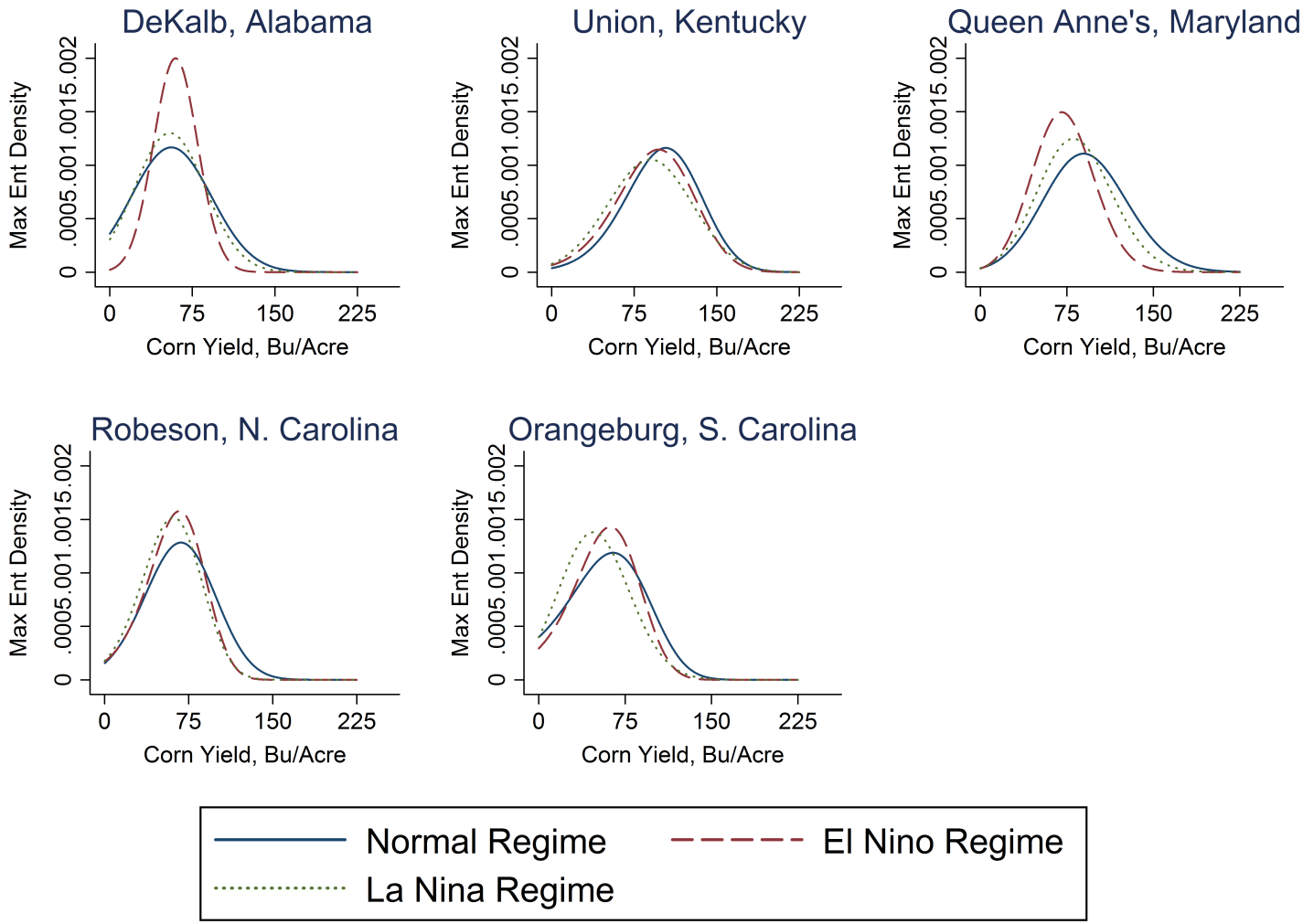

Figure 10: Yield Distributions in the Other Region

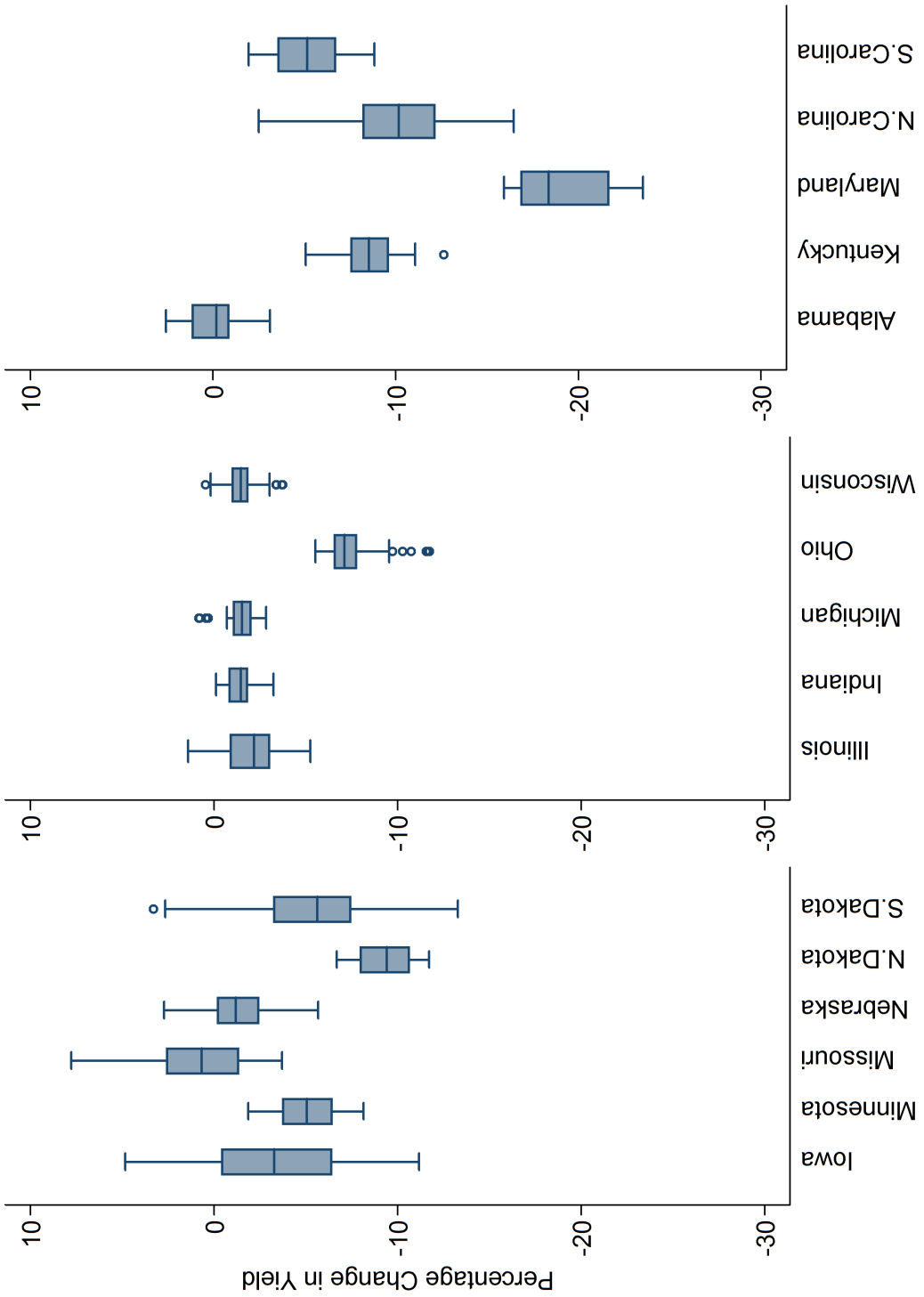

Figure 11: Box-Plots of County-Level Effects of El Niño on Mean Yields

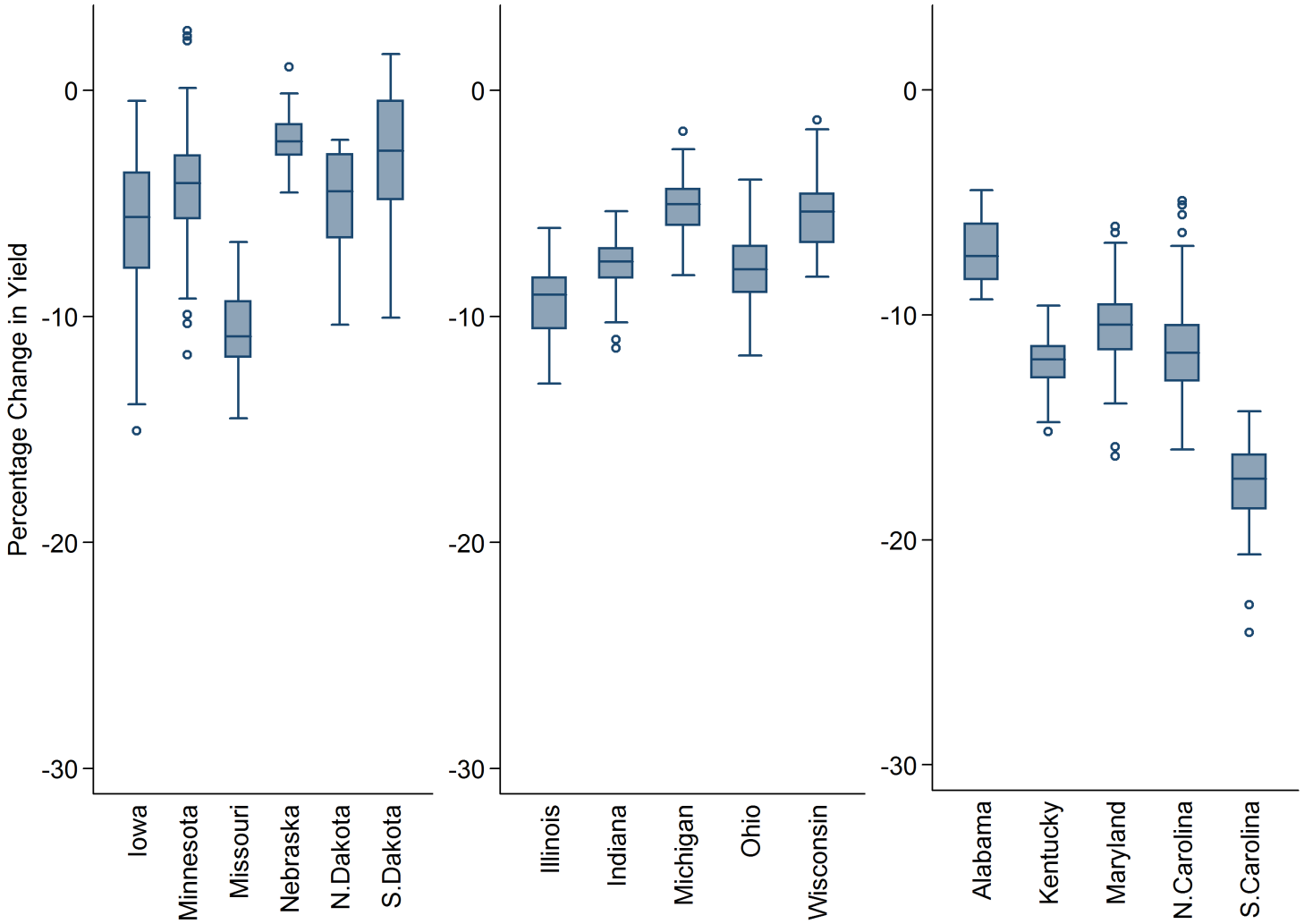

Figure 12: Box-Plots of County-Level Effects of La Niña on Mean Yields

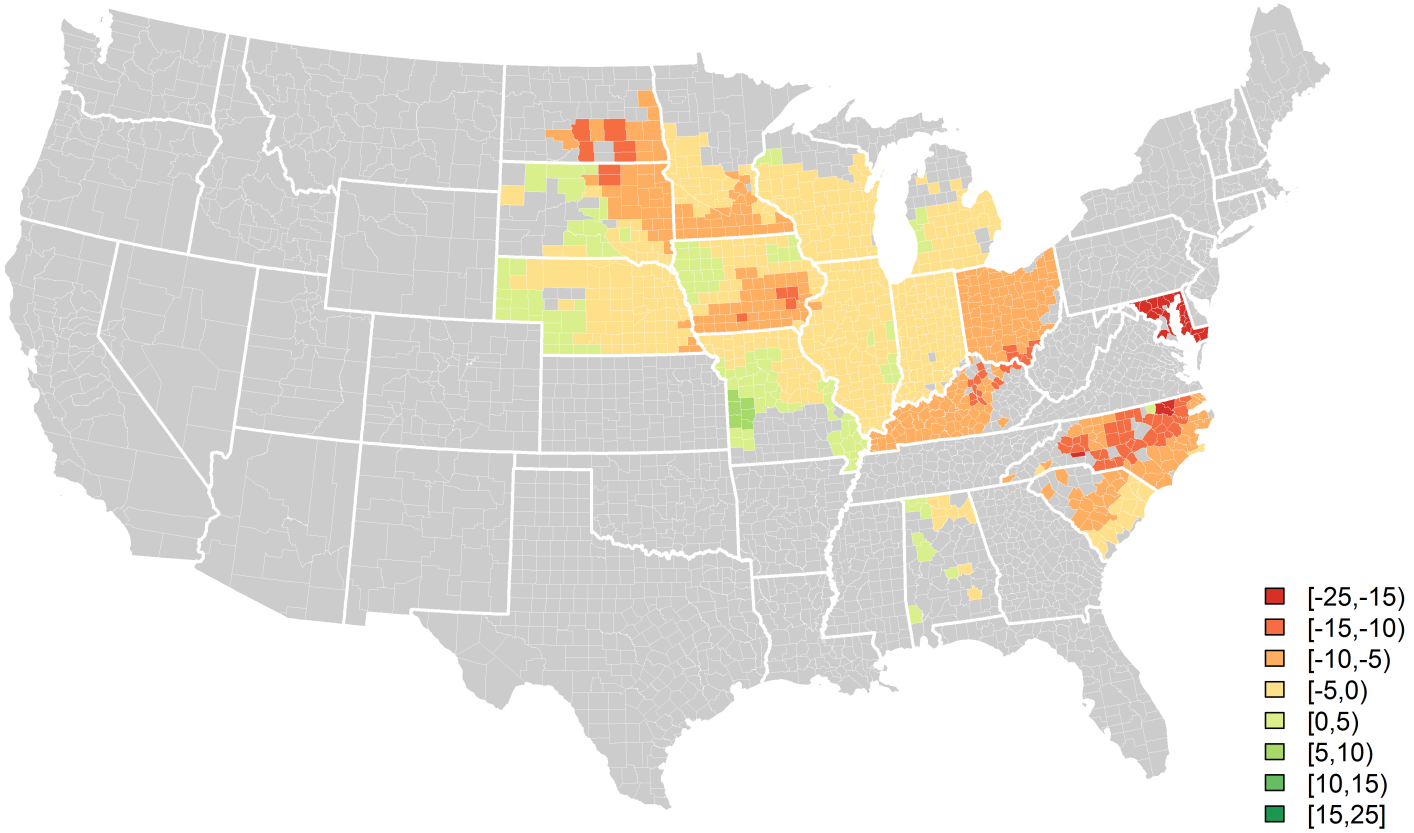

Figure 13: Spatial Representation of El Niño's Effect on Mean Yields

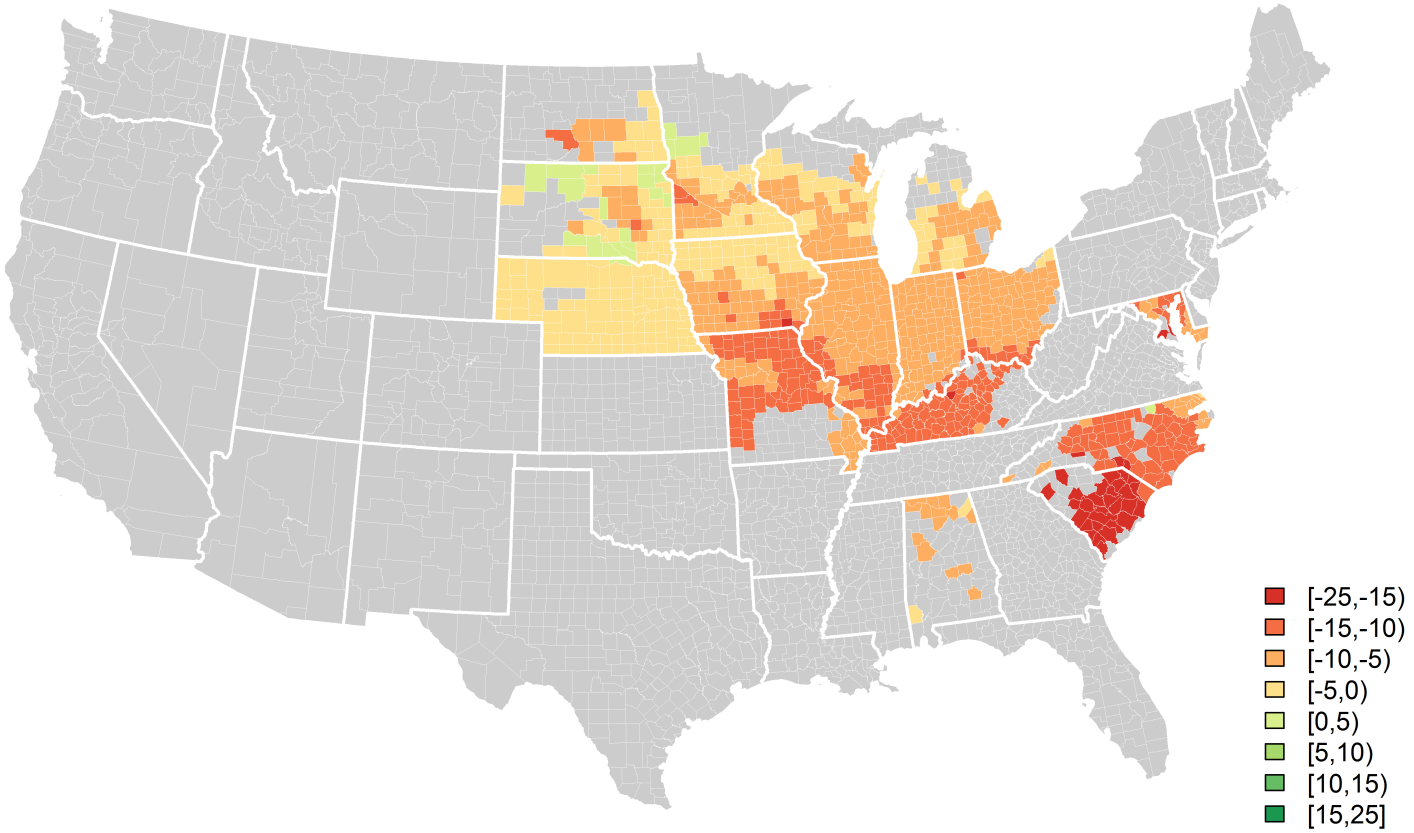

Figure 14: Spatial Representation of La Niña's Effect on Mean Yields

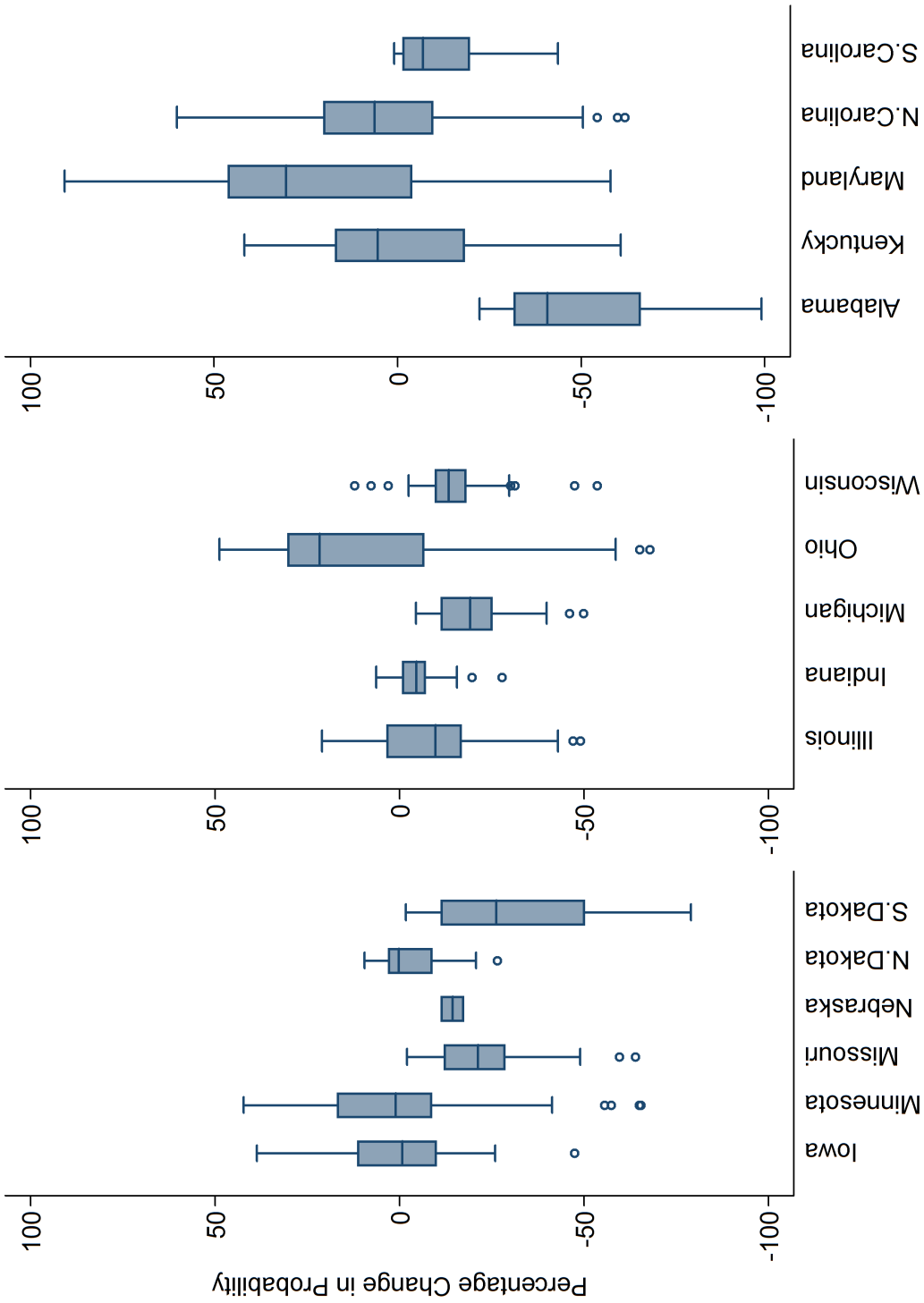

Figure 15: Box-Plots of County-Level Effects of El Niño on Downside Risk

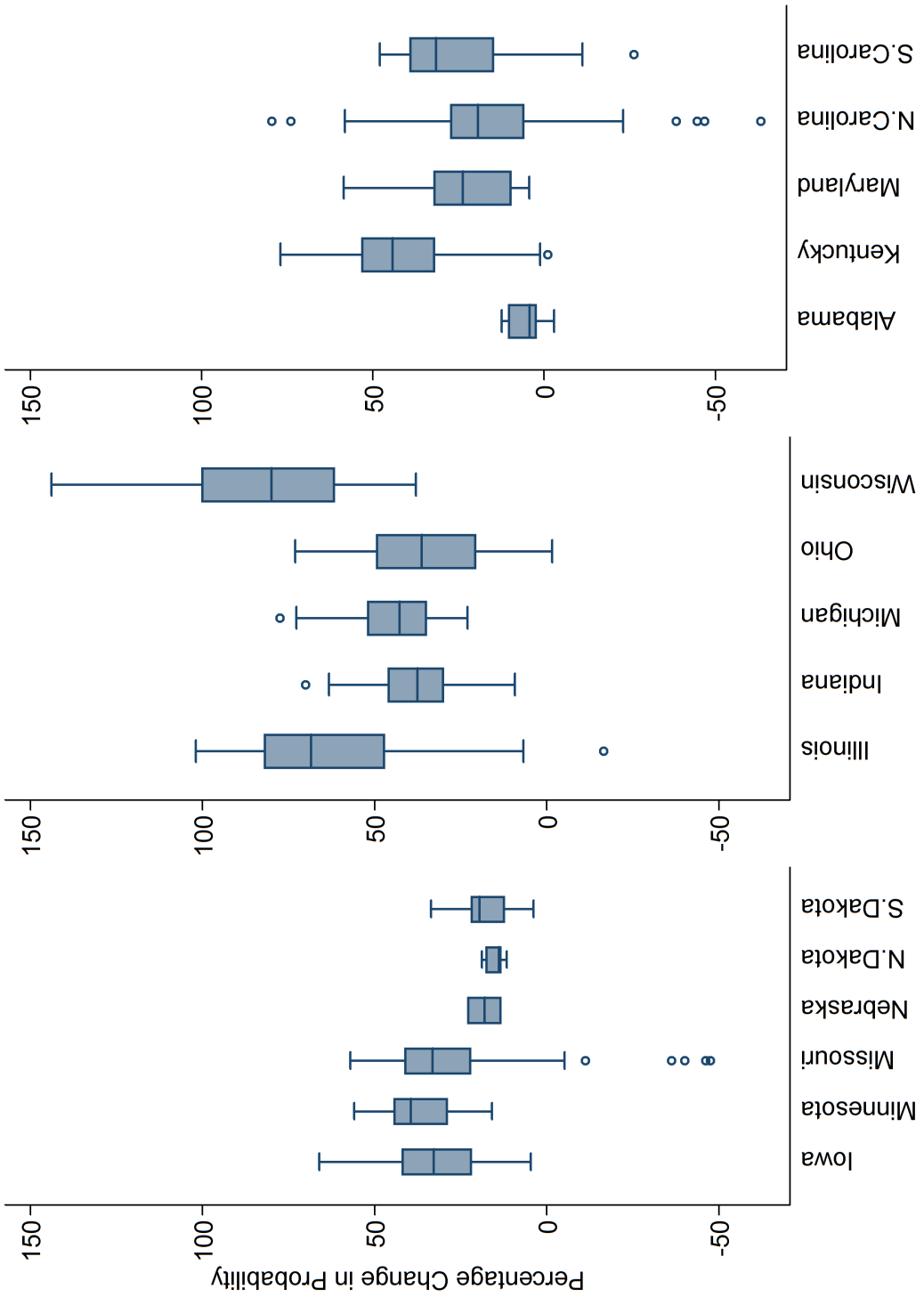

Figure 16: Box-Plots of County-Level Effects of La Niña on Downside Risk

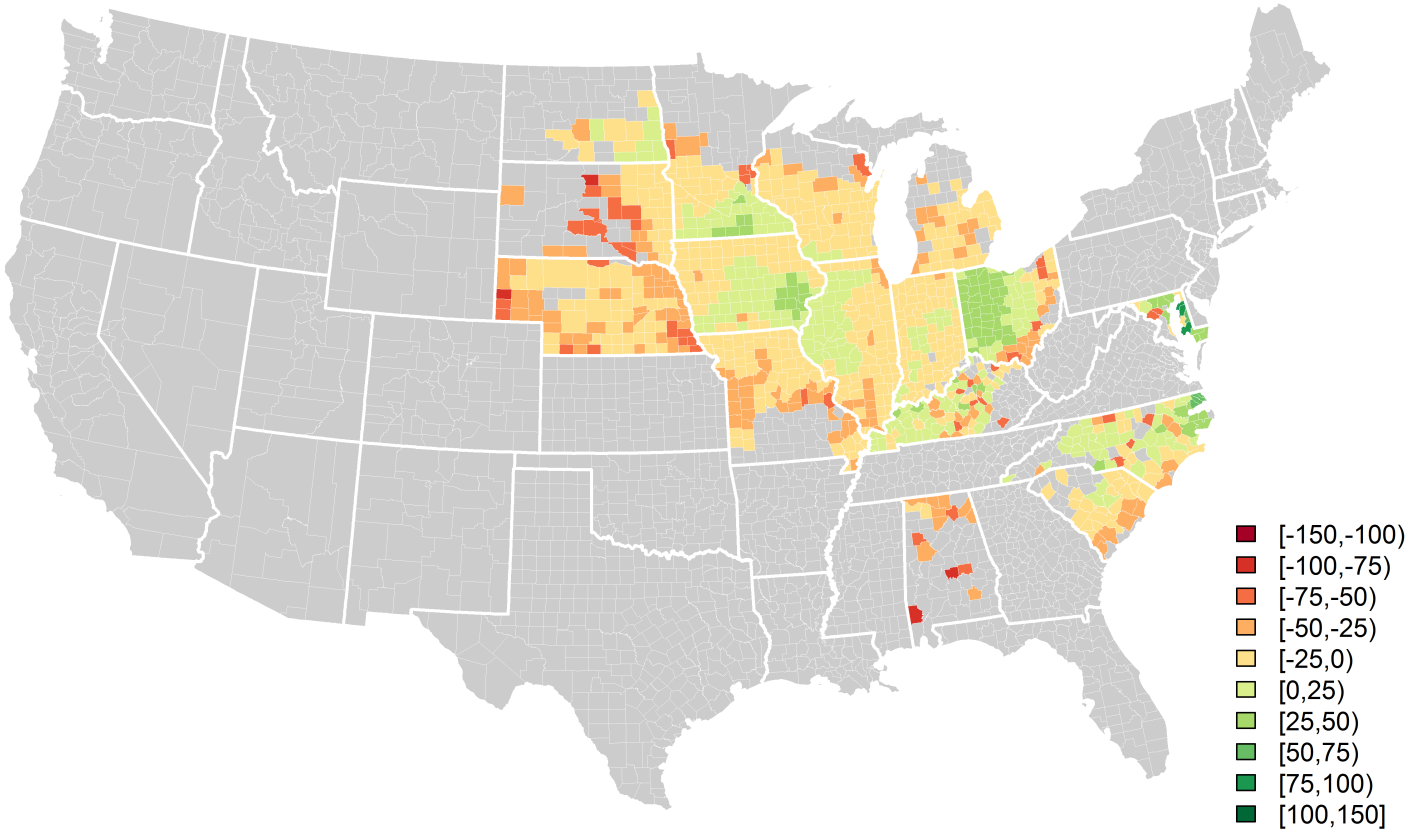

Figure 17: Spatial Representation of El Niño's Effect on Downside Risk

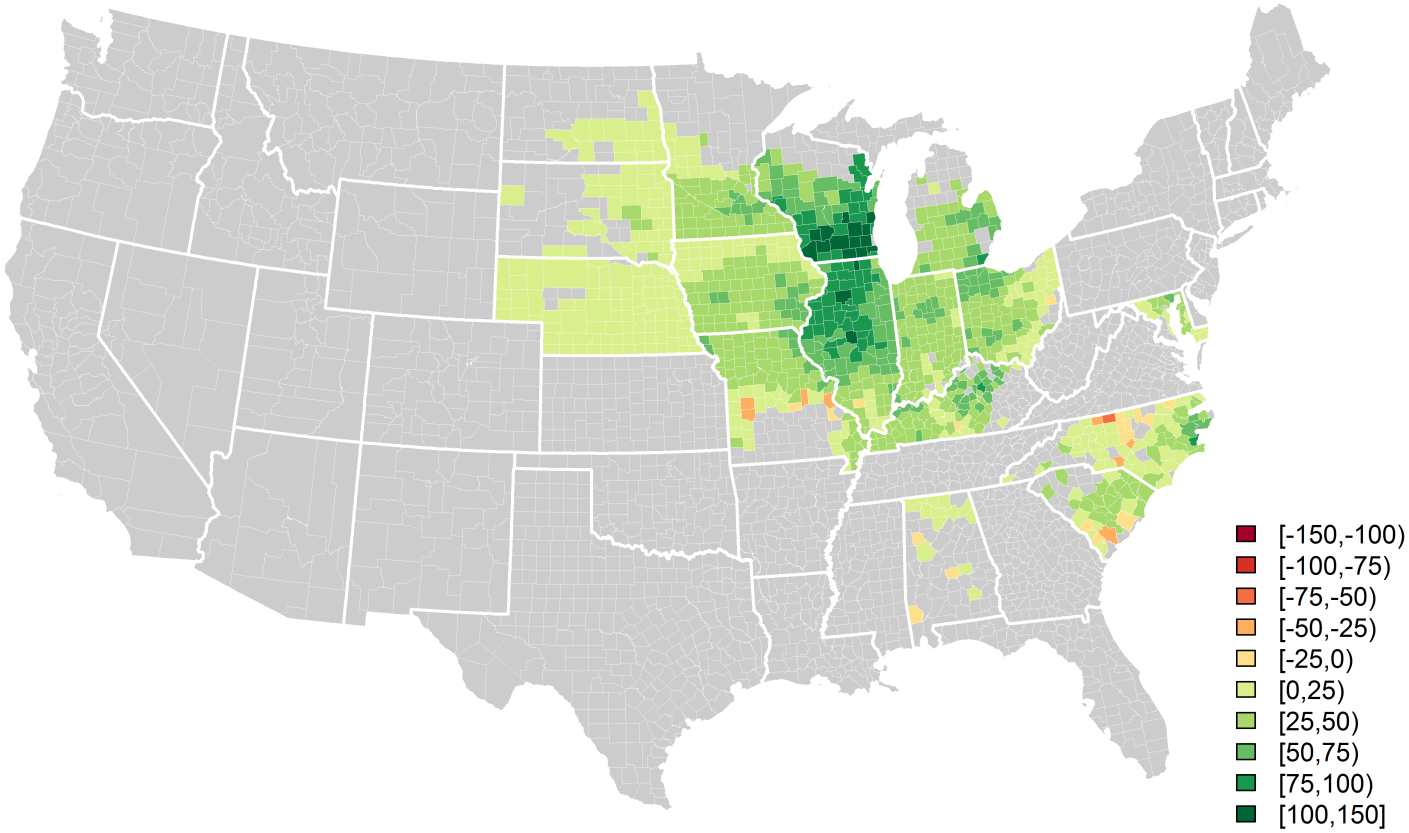

Figure 18: Spatial Representation of La Niña's Effect on Downside Risk